U.PORTO

UNIVERSIDADE DO PORTO

2.º CICLO M 2013

FEUP
2013

U.PORTO

Effect of the Nanohydroxyapatite Formulation NanoXIM•HAp102® on the Proliferation and Osteogenic Differentiation of Human Bone Mesenchymal Stem Cells

Elisabete Marina Nunes Pires

U.PORTO
FEUP FACULDADE DE ENGENHARIA
UNIVERSIDADE DO PORTO

Effect of the Nanohydroxyapatite Formulation NanoXIM•HAp102® on the Proliferation and Osteogenic Differentiation of Human Bone Mesenchymal Stem Cells

Elisabete Marina Nunes Pires

DISSERTAÇÃO DE MESTRADO APRESENTADA
À FACULDADE DE ENGENHARIA DA UNIVERSIDADE DO PORTO EM
MIB – Mestrado Integrado em Bioengenharia

Faculdade de Engenharia da Universidade do Porto

FEUP

Effect of the Nanohydroxyapatite Formulation NanoXIM•HAp102® on the Proliferation and Osteogenic Differentiation of Human Bone Mesenchymal Stem Cells

Elisabete Marina Nunes Pires

Dissertation performed under the
Integrated Master in Bioengineering- Biomedical Engineering

Supervisor: Prof. Doutora Maria Helena Fernandes (FMDUP)
Co-supervisor: Doutor Paulo Quadros (Fluidinova,S.A)

Porto, July 2013

Abstract

Tissue engineering approaches that are inspired in the hierarchical nanostructure of the bone have shown that this structure presents a higher reactivity and functional improvement when compared to microsized materials. Nanophase ceramics, especially nano-hydroxyapatite (nano-HA), are widely used for bone regeneration and/or replacement in many biomedical applications due to their great chemical similarity with bone and teeth and their documented ability to promote mineralization. Therefore, there is a strong interest for the syntheses of synthetic extra pure and well defined hydroxyapatite nanocrystals.

Fluidinova, Engenharia de Fluidos S.A, has developed and patented a novel continuous reactor, NETmix®, for nano-hydroxyapatite manufacture. This Netmix® technology allows the production of the nanoXIM•Hap102®. This product is a highly pure nanocrystalline hydroxyapatite in paste form, at 15% (weight/volume) in pure water, with promising features for bone regeneration.

This work aims to study the biological profile of the commercially available preparation nanoXIM•HAp102® regarding relevant cellular and molecular events involved in the proliferation/differentiation of human Mesenchymal Stem Cells (hMSCs).

Initially, a preliminary experiment was performed in order to select the appropriate concentration range of nano-HA to be tested in mesenchymal stem cells. Thereby, the dose-dependent effects of nano-HA were investigated in MG63 cells cultured for 7 days in the presence of nano-HA in the concentration range 1-1000 μg/mL, by evaluating the metabolic activity/cell proliferation by the MTT assay. Results of this preliminary experiment allowed to select the concentrations 1, 10, 50 and 100 μg/mL to evaluate the effect of nano-HA in hMSCs.

The response of hMSCs to nano-HA was characterized at days 7, 14 and 21 for cell viability/proliferation, histochemical staining of alkaline phosphatase (ALP) and collagen, apoptosis and expression of osteoblastic genes. In addition, cultures were observed by scanning electron microscope (SEM), confocal laser scanning microscopy (CLSM) and transmission electron microscopy (TEM).

The cell culture experiments showed negligible cytotoxicity of nano-HA in the range 1 - 50 μg/mL. In addition, the presence of nano-HA at 10 μg/mL caused an increase in the cell viability/proliferation, accompanied by the synthesis of ALP and collagen and a normal F-actin cytoskeleton organization, without any increase in the apoptosis rate. Moreover, hMSCs were able to increase the expression of BMP-2. The presence of higher nano-HA levels (50 and 100 μg/mL) were associated with slight deleterious effects in the measured cell response

parameters. TEM analyses revealed that nano-HA was readily internalized by hMSCs by endocytosis. Nano-HA aggregates were seen in varying size lysosomes and showed low intracellular dissolution rate.

In conclusion, these data contribute to further understanding of the functional properties of the nano-HA formulation NanoXIM•HAp102®. Accordingly, nano-HA was able to modulate the proliferation and osteoblastic differentiation of hMSCs. At selected conditions, nano-HA exhibits an interesting profile for bone tissue applications.

Resumo

Abordagens de engenharia de tecidos que são inspiradas na nanoestrutura hierárquica do osso têm mostrado que esta estrutura apresenta uma maior reatividade e desempenho funcional quando comparada com materiais micrométricos. Cerâmicos nanofásicos, especialmente a nano-hidroxiapatite (nano-HA), são amplamente usados na regeneração e /ou substituição óssea em muitas aplicações biomédicas, devido à sua grande similaridade química com o osso e os dentes; e devido à sua capacidade para promover a mineralização. Neste contexto, existe grande interesse em sintetizar hidroxiapatite sintética extra pura e com nanocristais bem definidos.

A "Fluidinova, Engenharia de Fluidos S.A", desenvolveu e patenteou um novo reator contínuo, NetMix®, para a fabricação de nano-hidroxiapatite. Esta tecnologia, NetMix®, permite a produção da nanoXIM•Hap102®. Este produto é uma hidroxiapatite nanocristalina de elevada pureza, comercializada na forma de pasta aquosa (15% peso/volume), com características promissoras para regeneração óssea.

Este trabalho tem como objetivo estudar o perfil biológico da preparação comercial nanoXIM•HAp102® relativamente a eventos celulares e moleculares pertinentes, envolvidos na proliferação e diferenciação osteoblástica de células estaminais mesenquimais humanas (hMSCs).

Inicialmente, foi realizada uma experiência preliminar com o objetivo de selecionar a gama de concentração apropriada de nano-HA a ser testada nas hMSCs. Desse modo, os efeitos dose-dependentes da nano-HA foram investigados em células osteoblásticas MG63, cultivadas durante 7 dias na presença de nano-HA na gama de concentrações de 1-1000 µg/mL, por avaliação da actividade metabólica/proliferação celular através do ensaio de MTT. Os resultados desta experiência preliminar permitiram determinar as concentrações de 1, 10, 50 e 100 µg/mL para avaliar o efeito da nano-HA em hMSCs.

A resposta das hMSCs à nano-HA foi caracterizada nos dias 7, 14 e 21 para a viabilidade celular/proliferação, coloração histoquímica da fosfatase alcalina e do colagénio, apoptose e expressão de genes osteoblásticos. Além disso, as culturas foram observadas por microscópia electrónica de varrimento, microscopia confocal de varrimento a laser e microscopia electrónica de transmissão.

Os resultados dos estudos celulares mostraram uma toxicidade mínima da nano-HA na gama 1 - 50 µg/mL. Além disso, a presença de 10 µg/mL nano-HA causou um aumento na viabilidade/proliferação celular, acompanhado pela síntese de fosfatase alcalina e de

colagénio, e por uma organização normal da actina-F do citoesqueleto, sem qualquer aumento na taxa de apoptose. Observou-se ainda um aumento na expressão de BMP-2. A presença de níveis mais elevados (50 and 100 μg/mL) causou um ligeiro efeito citotóxico, considerando os parâmetros avaliados. A observação das culturas por microscopia eletrónica de transmissão mostrou que a nano-HA foi rapidamente internalizada por um processo de endocitose. Observou-se a presença de agregados de nano-HA nos lisossomas, que mostraram uma taxa baixa de dissolução intracelular.

Em conclusão, este estudo contribui para uma melhor compreensão das propriedades funcionais da formulação NanoXIM•HAp102®. Assim, a nano-HA apresentou capacidade de modular a proliferação e a diferenciação osteoblástica de células mesenquimais humanas. Em condições apropriadas, a nano-HA exibe um perfil interessante para aplicações no tecido ósseo.

Acknowledgements

First of all I would like to express my sincere gratitude to Prof. Doutora Maria Helena Fernandes, my supervisor, for giving me opportunity to undertake this work, for all her support, advices and encouragement. Her contributions, detailed comments and insight have been of great value to me.

I thank “Fluidinova, Engenharia de Fluidos S.A”, especially Dr.Doutor Paulo Quadros, by had provideding the productnanohydroxyapatite particles for his this study, and for the support he provided at different levelsduring this work.I also would like to thank to Prof. Doutor Fernando Jorge Monteiro for helping me to look for a project.

My sincere thanks to Prof. Doutor Pedro Gomes and Doutora Mónica Garcia, at “Laboratory for Bone Metabolism and Regeneration”, for their support, all the comments and working suggestions; it helped me being a better student.

Prof José Duarte of Faculdade de Desporto, Universidade do Porto, for scientific support in the characterization of the samples for TEM analysis.

To my friends and colleagues, Diogo Constante, Diogo Neto and Joana Santos, my genuine recognition for the friendship, encouragement and really good moments of laugh.

I express many thanks and affection to my parents, brother and sister to whom I own what I am.

Finally, I wish to thank my boyfriend, Nuno Machado, for his true love, patience and understanding in this moment of my life. Moreover, I thank you for the never-ending support, words of advice and for always being there for me, during this long term journey.

Contents

List of Figures

List of Abbreviations

ALP	Alkaline phosphatase
BMPs	Bone morphogenic proteins
BMU	Basic multicellular units
BSP	Bone sialoprotein
CaP	Calcium phosphate
CDNAs	Complementary DNAs
CLSM	Confocal Laser Scanning Microscopy
Col I	Type I collagen
DHA	Calcium deficient hydroxyapatite
DMSO	Dimethyl sulphoxide
dNTPS	Deoxynucleotide triphosphates
ECM	Extracellular matrix
FEUP	Faculdade de Engenharia da Universidade do Porto
GAPDH	Glyceraldehyde-3-phosphate dehydrogenase
HA	Hydroxyapatite
hMSCs	Human mesenchymal stem cells
ID	Integrated density
Micro-HA	Microphase hydroxyapatite
MRI	Magnetic resonance imaging
MSCs	Mesenchymal stem cells
Nano-HA	Nanoscale hydroxyapatite
OC	Osteoclacin
OP	Osteopontin
OPG	Osteoprotegerin
PBS	Phosphate-buffered saline
PF	Primers sequence forward
PFA	Paraformaldehyde
PR	Primers sequence forward reverse
RANKL	Receptor activator of nuclear factor kappa B ligand
RT-PCR	Reverse transcription-polymerase chain reaction
Runx-2	Runt related protein 2
SEM	Scanning Electron Microscope
TEM	Transmission electron microscopy
Wnts	Wingless-ints pathway
α-MEM	α-minimal essential medium

Chapter 1

Introduction

In bone regeneration, the success of using materials with nanosized features, namely hydroxyapatite (HA), comparatively to microstructure materials, is considerable. These nanomaterials can be used as nanocomposites containing dispersed nanosized calcium phosphate (CaP) and, also, as simple nanoscale grains [1]. The reason for the success of nanomaterials in bone applications is because they display unique physical and chemical properties. Decreasing material size into the nanoscale, it dramatically increases surface area, surface roughness and surface area to volume ratios [1-3]. Thus, these materials represent an increasingly important material in the development of novel materials which can be used in numerous applications.

When a material is implanted in the bone tissue, the osteointegration process is influenced by the properties of the material surface (as topography and chemistry), that have the ability to modulate the molecular and cellular events at the implant interface. Nanomaterials with surface properties similar to the bone are undoubtedly appropriate for the bone regeneration and, therefore, are expected to improve orthopaedic/dental implant efficacy [4].

Nanophase ceramics, especially nano-hydroxyapatite (nano-HA), are widely used for bone regeneration and/or replacement in many biomedical applications due to their documented ability to promote mineralization [2]. Synthetic HA is a CaP with the chemical formulae $Ca_{10}(PO_4)_6(OH)_2$, which is similar to the principal inorganic constituent of bone and teeth [3,5].

Synthetic nano-HA can be produced using two routes, i.e. dry and wet methodologies. Fluidinova has a new technology to produce nano-HA, the NETmix® technology. By this technology, the Fluidinova developed and patented an industrial process based on the wet chemical reaction for controlling, at the molecular level, the calcium and phosphate reaction to produce HA nanoparticles [6], thus creating a novel product - nanoXIM•Hap102®. This product provides promising features for bone regeneration, as bone tissue engineering strategies might involve the use of synthetic nano-HA and precursor cells with the ability to differentiate into the osteogenic lineage.

1.1 - Thesis Objectives and Layout

For bone regeneration has been increasing much investigation for materials to replace bone defect over last decades. This thesis aims to study biological profile of the commercially available preparation nanoXIM•HAp102® regarding relevant cellular and molecular events involved in the proliferation/differentiation behaviour of human Mesenchymal Stem Cells (hMSCs).

This synthetic HA, in a paste form, is the focus of this work, as the HA nanoparticles present in this paste are a very promising material for bone regeneration strategies [6]. In this context, the main objective of the work described in this thesis is to acquire information on the interaction of these nano-HA particles with human mesenchymal stem cells, which is essential to their application in bone tissue engineering. Therefore, it is intended to obtain integrated information on the uptake and intracellular fate of HA nanoparticles by hMSCs and the elicited cell response regarding proliferation and differentiation events.

The layout of the present work is divided as follows. In Chapter 2 the state-of-the-art, on the prospective use of nano-HA in bone regeneration and, also, to overview the most recent developments in this field. Moreover, it reports the relevant cellular processes occurring in bone tissue during normal metabolism and regeneration events, as well as general background on mesenchymal stem cells, which can be used to study the suitability of a material for bone regeneration approaches. In summary, the contents addressed have a fundamental aim to provide background for a rational intervention in this work.

The experimental methodology is described in Chapter 3. Results are presented in Chapter 4, and discussed in Chapter 5. Finally, the general conclusions drawn from this work are presented in Chapter 6.

Chapter 2

Literature Review

2.1 - Tissue engineering

Tissue engineering is an emerging field of interdisciplinary science and research that encompass several scientific areas such as medicine, biochemistry and materials science. It generally involves the use of materials and cells with goal of trying to understand tissue function and restore of damage tissues. In summary, it aims at developing new approaches for encouraging tissue growth and repair. [7-10]

Nowadays, there are several bone pathological conditions that might require the use of biomaterials to restore bone structure and function, such as bone fracture, osteoporosis, and bone cancer, among others. However, traditional implant materials may be associated with several complications, namely failures originating from implant loosening, inflammation, infection, osteolysis and wear debris. Bone tissue engineering has a major role in bone repair approaches, particularly by using nanotechnology, which becomes obvious when examining nature. [2]

With the entry of the nanotechnology in the field of regenerative medicine, there are many developments of nanostructured biomaterials, which have the ability for guiding cellular behaviour by presenting specific morphological and biological cues [1].

Accordingly in bone tissue engineering, one of the main interests is the development of novel nanomaterials with appropriate mechanical properties and, also, biomimetic in terms of their nanostructure [1-3].

Therefore, bone tissue engineering develops new approaches inspired by the hierarchical nanostructure of bone. This approach intends to obtain adequate synthetic nanomaterials (such as calcium material bioceramics) that should ideally be biocompatible, osteocondutive, osteoinductive, osteogenic, and biodegradable, leading to osteointegration [1].

2.2 - Bone

2.2.1 - Bone function

Bone is a living conjunctive tissue in permanent growth, since throughout life it is constantly removed and replaced [11]. It has the mechanical function of providing attachment for muscles, facilitating the locomotion process, and it provides structural support for the other systems and organs [11-13]. Furthermore, bone is considered as a reservoir of calcium, phosphate and other inorganic ions [14].

2.2.2 - Bone composition

Bone is a composite material, constituted by bone cells dispersed in a bone matrix, which has an organic and a mineral component. The organic part of this matrix is mainly composed of fibrillar collagen type I (~90%) and noncallagenous proteins (10%) such as osteonectin, osteocalcin, osteopontin, bone sialoprotein, proteoglycans, glycoproteins, enzymes (e.g. alkaline phosphatase) and cytokines [1, 15]. The mineral phase of mature bone tissue is composed by calcium and phosphate. This phase has many similarities to the synthetic hydroxyapatite (HA), which has the chemical structure $Ca_{10}(PO_4)_6(OH)_2$ [3]. The bone mineral phase also contains other ions, such as carbonate, citrate, sodium, magnesium, fluoride, hydroxyl, potassium and others that can be found in smaller amounts [15, 16].

2.2.3 - Bone Structure

The morphological structure of the bone can be classified as cancellous (spongy or trabecular bone) and as cortical (compact or dense bone) [11]. Both types of bone exist in different proportions in several locations of de skeleton.

The compact bone is dense and it is located on the external parts of the bone. Its main function is to provide strength, it is relatively acellular and it has low metabolic activity [17]. Cortical bone is organized in cylindrical units, Haversian systems also known as osteons, which forms the diaphysis of long bones [15]. The Haversian systems are surrounded by a concentric layer of rings or lamellae [13, 15]. In the inner of the lamellae there are tiny spaces called lacunae containing bone cells, the osteocytes [13]. These units are considered the structural units of this type of bone. Osteons are typically circular or oval in cross section, 20 to 110 μm in diameter, and contain central canals with blood vessels to provide nutrition, lymph vessels and occasionally nerves [11, 13, 17]. The intercommunicating pore systems, constituted by canaliculi, lacunae and Volksmann's canals which connect with Haversian canals, allow the transport of metabolic substances [15, 17].

Cancellous bone is porous and it is sited in the interior of bone. In general, cancellous bone is more closely associated with metabolic processes [11, 15]. It is found in the epiphysis of bone and this type of bone is lamellar in structure. The microstructure of cancellous bone shows interconnecting rods or occasionally plates of bone called trabecular [11, 13]. Cancellous bone is arranged as open cell porous networks that allow the transport of metabolic substances [15].

The periosteum is the membrane that covers bone external surface, not including the articulating joints. It consists of an outer fibrous layer containing collagen fibres and fibroblasts and an inner layer that contains the osteogenic cells [12, 13, 18]. The inner surface of the bone is covered by a thin membrane called the endosteum. This membrane is found facing the medullary cavity. The endosteum contains a single layer of cells and a small amount of connective tissue [18]. Both lining membranes, periosteum and endosteum, contain osteoblasts and their progenitor cells [13].

2.2.4 - Bone cells

Bone tissue is dynamic organ undergoing constant remodelling. This is possible to the important role of bone cells. These cells are responsible for producing, maintaining and modifying the bone tissue in order to maintain its mechanical and structural properties [11]. There are four types of cells in bone tissue: osteoblasts, bone lining cells, osteocytes, and osteoclasts (figure 1) [11, 18]. Osteoblasts, osteoclasts and bone lining cells, that are located on the bone surfaces, and osteocytes, that can only be found in the interior of the mineralized extracellular matrix (ECM) [11].

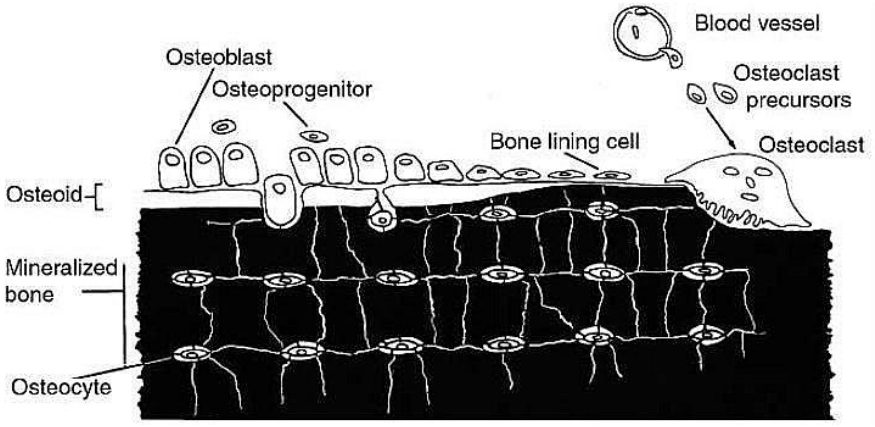

Figure 1 - The origins and locations of bone cells *(Adopted from Downeyet et. al 2006)*.

2.2.4.1 - Osteoblast

Osteoblasts are mononuclear and differentiated cells, with low mobility and their function is to synthesize the bone matrix and regulate the mineralization of the osteoid [15, 19]. Therefore, the osteoblasts are responsible for bone building because they play an active role in the synthesis of the proteins and polysaccharides of the bone matrix [20]. When active, osteoblasts have a characteristic morphology, since they have a marked cytoplasmic basophilia, round nuclei rich in ribonucleic acid located at the base of the cell opposite to the bone surface, contain large quantities of rough endoplasmic reticula, and the Golgi apparatus is a well visible, features typical of a protein producing cell [21-23].

Osteoblasts, during their lifetime, have several fates. They can follow one of three pathways: (1) remain active osteoblasts, (2) become surrounded by matrix and become osteocytes, or (3) transform into the relatively inactive bone lining cells [21, 24]. Briefly, osteoblasts may disappear by transformation into either bone-lining cells or osteocytes, or even by apoptosis mechanisms [20].

The osteoblast cells originated from undifferentiated mesenchymal stem cells (MSCs) that have the potential to become osteoblasts. MSCs are found in bone canals, endosteum, periosteum and marrow [11, 21, 25]. The undifferentiated cells remain in this state until they are stimulated to proliferate and differentiate into the osteoblast, thus MSCs behave as a pre-osteoblast, and they can migrate from neighbouring tissues or through the vascular system up to a target site [11, 21, 22, 26]. The osteogenic cells, MSCs, can be induced to differentiate into osteoblasts producing a bone like matrix by the synthetic glucocorticoid, dexamethasone, or by the bone morphogenic proteins (BMPs) [27]. Differentiation of MSCs into osteoblast cells is controlled by the regulated expression of genes that define three main periods of osteoblast phenotype development (proliferation, extracellular matrix (ECM) development and maturation, and mineralization). During proliferation, several ECM proteins, such as histone H4 and type I collagen (Col I) can be detected in this stage. Expression of alkaline phosphatase (ALP) is an earlier marker of the matrix maturation phase, while the expression of osteopontin (OP) and osteocalcin (OC) is found in the late maturation or early mineralization phases [23, 27].

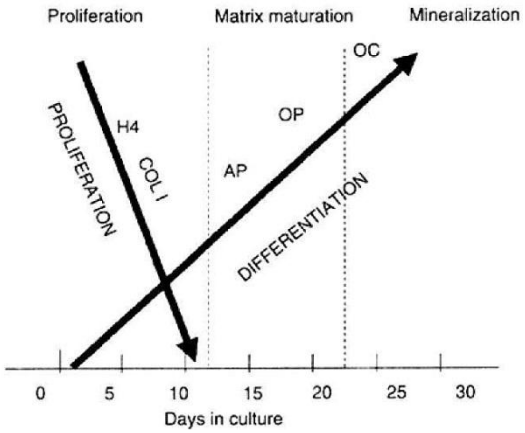

Figure 2 - The relationship between cell growth and differentiation-related gene expression during development in culture of the osteoblast phenotype: histone H4, COL I, ALP, OP, OC. The three principal stages of the osteoblast developmental are shown: proliferation, ECM development and maturation, and mineralization. *(Adopted from Lian et. al 1995).*

2.2.4.2 - Bone lining cells

Bone lining cells are inactive osteoblasts with flat appearance that cover most of the surface area of the normal bone [11, 21]. These cells are considered to be in communication with osteocytes and are found linked to each other, through cytoplasmic extensions or gap junctions [21].

The functions of the bone lining cells include the protection of the bone from the extracellular fluids, maintaining the bone own environment, the response to mechanical forces on the skeleton [21, 24] and, also, to several hormones, playing a role in the bone remodelling events [11, 20-22]. In addition, they are involved in mineral homeostasis, namely in the exchange of calcium and phosphorus ions into and out of the bone [11, 20].

2.2.4.3 - Osteocytes

The osteocytes are mature bone cells, and are the main cells in bone tissue (>90%) [11, 18, 21, 22, 24]. These bone cells are spidery in shape with a plump cell body and reside in a lacuna, and the slender cytoplasm processes that radiate from osteocytes are found in canaliculi [11, 21]. In general, the osteocytes are surrounded by bone matrix, thus they have small nuclei, scanty cytoplasm with mitochondria and a small Golgi zone indicating their low activity compared to the osteoblasts [11, 22]. An osteocyte may derive from the osteoblast that became embedded in its own osteoid [11].

The function of this cell is to maintain the bone tissue, being involved in the exchange of nutrients and wastes with the blood. Like osteoblasts, osteocytes do not undergo cell division. [18]~

2.2.4.4 – Osteoclasts

The osteoclasts are multinucleated giant cells differentiated from the monocyte/macrophage lineage, wherein are formed to carry out the unique function of bone resorption under both normal and pathological conditions. [11, 13, 21]. Once the osteoclasts are derived from a monocyte stem-cell lineage, they are equipped with phagocytic-like mechanisms similar to circulating macrophages. So, following osteoclast attachment to the bone surface, bone degradations begins by direct chemical and enzymatic attack [12].

Morphologically, the osteoclast can have several forms because they have a high mobility, moving from various sites and along the bone surface [21]. In general, these cells are found at the surface of bone and they may be much larger than other bone cells, because they might contain up to 50 nuclei [11, 21].

2.2.5 - Bone remodelling, healing and repair

Bone is constantly being remodelled by the highly regulated bone resorption and forming actions of the osteoclasts and osteoblasts, respectively [11, 13]. Thus, the bone is found throughout life in remodelling, i.e. bone has a continuous shaping. As the old bone is removed, new bone is produced to replace it, and calcium ions are released for other tissues [11, 18].

The processes involved in the bone replacement, bone reabsorption and bone formation, are regarded as independent events, but according to Frost [28] that described the sequential activities of bone replacement, they are closely linked spatially, in an anatomical and temporal sequence, to ensure a balance in the removal of mineralized matrix and the bone replacement [11, 29]. The anatomical structure is named basic multicellular unit (BMU), and this structure describes the sequential activities of osteoclasts and osteoblasts during remodelling [29].

In the process of bone reabsorption, the osteoclasts adhere strongly to the bone surface at the endosteum or periosteum, and releases protein-digesting lysosomal enzymes and several acids into the sealed surface. Thereby, the collagen fibres and other organic substances are digested by enzymes, while the acids dissolve the bone minerals. The degradation products of the bone, mainly calcium and phosphorus, go to the bloodstream by

exocytosis. Thus, bone remodelling occurs when the small area removed by the osteoclasts is rebuilt by the osteoblasts [18].

The remodelling rate for compact bone is about 4% per year, and for spongy bone it is about 20% per year [18, 30]. However, the bone remodelling can also take place at different rates in different regions of the body [30].

The bone remodelling process allows the removal and the repair of bone microdamage, the adaptation to mechanical stress and the maintenance of its strength and integrity [18, 31]. Furthermore, the skeletal remodelling maintains the mineral ion homeostasis. Remodelling is regulated and stimulated by a number of hormones, such as vitamin D, parathyroid hormone, calcitonin and estrogen [24].

Injury in the bone, such as a fracture or the implant replacement, results in the loss of continuity of bone tissue, and it is associated to the damage of the blood vessels. Consequently, haemorrhage occurs and there is the formation of a blood clot, or hematoma [33]. Healing of bone tissue provides the capacity to repair the tissue continuity, form and function with a mechanism scar free [34, 35]. Bone tissue has a potential to heal itself, resulting in the regeneration of the anatomy of the bone and complete function.

The bone repair process is very complex, because it involves the coordination and sequence of many biological events [35, 36]. Bone healing can be divided into four phases: blood clotting, inflammatory phase, reparative phase and remodelling phase [34-36].

Once the bone tissue injury leads to damage to surrounding tissues, the bone healing is initiated by the activation of the coagulation cascade and by the formation of the blood clot [35, 36]. The blood clot allows the cellular migration and proliferation; furthermore, it functions as a primary source of growth factors [34]. Thus, inflammatory cells are recruited, such as neutrophils, macrophages, monocytes, lymphocytes, and cells of other lineages, such as fibroblasts and endothelial cells. Then, recruitment of the cells is followed by an acute inflammatory response resulting in the edema and cytokine and growth factor release [36].

The healing process continues by the reparative phase with resorption of the blood clot and its replacement by the deposition and formation of granulation tissue [34]. In this phase, there is vascular growth and migration of osteogenic cells. The granulation tissue is responsible for providing blood supply and for the recruitment of undifferentiated mesenchymal stem cells. At the lesion site, these cells proliferate and differentiate because they responded to growth factors released by the injured tissues and from the clot [3]. Finally, after 6 to 8 weeks, bone tissue is completely remodelled in the original shape, structure, function and mechanical properties [34, 35].

2.3 - Bone marrow and stromal cells

Bone marrow is a very complex organ, and it is composed by stromal tissue, hematopoietic cords and sinusoidal capillaries [36, 37]. The stromal tissue supports haematopoiesis and is made up of a network of extracellular matrix and cells [36, 38, 39]. Furthermore, stromal tissue has well known osteogenic potential [40].

Bone marrow stromal cells are widely used in tissue engineering [40, 41]. These cells are a heterogeneous population of non-hematopoietic cells of mesenchymal origin and fibroblastic cells [36, 40, 41]. Other cells are present in this population, such as monocytes, macrophages and endothelial cells [36, 40]. Following the culture of bone marrow stromal cells, the non-adherent cells are removed after medium change and cell passage [41].

Included in the adherent cell population, the mesenchymal stem cells (MSCs) are multipotent cells widely used in tissue engineering.

2.3.1 - Mesenchymal Stem Cells

The MSCs have the capacity of self-renewal and they are defined as a type of adult stem cells which contribute, in some circumstance, to the regeneration of mesenchymal tissues, once they can produce progeny that differentiate across the three primary germ layers (ectoderm, mesoderm and endoderm) [36, 42, 43]. Human MSC are easy to isolate from small aspirate of bone marrow via their adherence ability and they can be easily expanded in vitro [39].

MSCs that can give rise to mature cells, and in defined in vitro conditions, these cells readily differentiate to multiple connective tissue lineages, including osteoblasts, chondrocytes, and adipocytes [39, 43].

The morphology of the MSCs is characterized by a small cell body with a few cell processes that are long and thin. Furthermore, MSCs have a nucleus with prominent nucleolus which is surrounded by finely dispersed chromatin particles, giving the nucleus a clear appearance [20].

These cells are widely used in tissue engineering, because the selection of the culture conditions and the subsequent manipulations allow defining cell differentiation.

2.3.2 - Osteogenic differentiation potential of MSCs

The in vitro expansion of MSCs has been extensively studied by tissue engineering owing to their potential to differentiate into osteogenic tissue. The osteoblastic behaviour of MSCs in culture is normally achieved by culturing in an appropriate standard cell culture medium (i.e., α-minimum essential medium with 10% foetal bovine serum) supplemented with β-glicerophosphate, ascorbic acid and dexamethasone [27, 44-46]. Under these conditions, the MSCs in culture acquire an osteoblastic morphology and differentiate along the osteogenic phenotype, being able to express typical osteoblastic genes and to form a collagenous mineralized matrix [45, 46].

2.3.2.1 - Gene expression of MSCs during osteogenic differentiation

The MSCs have a potential to generate many cellular lineages such as osteogenic, adipogenic or chondrogenic cell lineage [47, 48]. The differentiation of MSCs into a cell lineage is dependent on the activated signalling pathways and several transcription factors [13, 47, 49, 50].

The transcriptional factors runt related protein 2 (Runx-2), osterix and β-catenin are essential to regulate the differentiation of MSCs into osteoblast lineage [47].

Osteoblast commitment and differentiation are guaranteed by Runx-2, it is responsible for inducing the osteogenic phenotype at an early stage and also to inhibit the differentiation of MSCs into adipocytes and chondrocytes [13, 47, 49, 51]. Runx-2 is known to activate and up-regulate the expression of major bone matrix protein genes of osteoblast differentiation, such as type I collagen (Col I), osteopontin (OP), bone sialoprotein (BSP) and osteocalcin (OC)

[47, 49, 52]. Therefore, this transcriptional factor allows cells acquiring an osteoblast phenotype, although keeping the osteoblast cells in an immature stage, the preosteoblast [47, 49]. Preosteoblast proliferation and differentiation follows distinct phases: preosteoblast, mature osteoblast, and osteocyte, which are regulated by transcription factors and express specific phenotypic genes [53].

Other factors can regulate the activity of specific transcription factors maintaining an osteoblastic fate. They include bone morphogenetic proteins (BMPs) that are recognized for their osteoinductive proprieties, and regulate the differentiation of MSCs into osteoblasts components of bone [49]. Furthermore BMP-2 and wingless-ints (Wnts) pathways together have a critical role in promoting Runx-2 expression to promote osteoblast differentiation [13, 51].

The osteoblastic phenotype is characterized by the synthesis of specific bone proteins that define a genic expression pattern. The gene markers expression of osteoblast allows defining the distinct stages of osteoblast phenotype development: proliferation, matrix maturation and mineralization. In each stage there are characteristic changes in gene expression [49, 54, 55].

As already mentioned, in an early stage during the proliferative phase, there is the expression of genes that support the proliferation, such as Col I and fibronectin [23, 27, 49, 56]. However, in this phase, BMP-2 and BMP-5 have a significant role in increasing ALP activity and OC synthesis [49]. So, the accumulation of these matrix proteins allows, in part, the end of cell proliferation. The differentiation stage is recognized by early cell differentiation that is characterised by the transcription and expression of the ALP [56]. Thereby, these markers are widely used to evaluate the osteogenic differentiation. Ultimately, the ECM becomes into the mineralization phase in which osteoblastic cell express osteopontin (OP) and osteocalcin (OC). These protein markers are found in the late maturation or early mineralization phases [23, 27, 49].

Osteoblasts produce osteoprotegerin (OPG) which is a soluble decoy receptor for the receptor activator of nuclear factor kappa B ligand (RANKL), and it is known that the major effect of OPG is to inhibit osteoclastogenesis [50, 57]. However, its role in osteoblast differentiation is still unclear. More recently, *Yu et al. (2011)* showed that OPG expression is associated with preosteoblast maturation and promotes matrix maturation [57].

In a study on osteoblast behaviour or osteogenic differentiation of MSCs it is very important to analyse the gene expression profile of the cells. The interest in analysing the RNA is explained by a cell's ability to adjust its mRNA copy numbers in response to environmental changes, being a crucial element in the complex regulation of gene expression. Moreover, at the mRNA level, it is known that a wide spectrum of pathological processes is associated with changes in gene expression [58].

The reverse transcription-polymerase chain reaction (RT-PCR) is a powerful tool for gene expression analysis. This technique is a PCR method that uses reverse transcriptase enzymes for making DNA from RNA [59]. The RT-PCR combines synthesis of the cDNA with its amplification allowing the cloning of genes from its mRNA. Thereby, this technique allows the analysis of the gene expression [59]. The result obtained from RT-PCR analysis allows to know whether a specific gene is being express into a cell [59].

The PCR method is characterized by the ability of DNA polymerase enzyme to synthetize a new strand of complementary DNA. The PCR reaction requires: a biological sample that contains DNA or RNA; a DNA polymerase enzyme; some salts for the DNA polymerase to

function; deoxynucleotide triphosphates (dNTPS) which provide essential nucleotides for new DNA strands; and finally oligonucleotides primers, which are responsible for initiating the chain reaction, being extremely specific to the precise genetic sequence of interest [59-61]. After PCR reaction, the reaction components are placed into a thermocycler, where they undergo basic PCR steps [59]. The PCR procedure involves repeated cycles of three steps, namely heat denaturation, annealing, and primer extension [59, 62].

In the first step, the thermocycler drives the reaction components up to denaturation temperature, typically 92 to 94°C. The denaturation allows that the hydrogen bonds of the double DNA helix are broken, and thereby the DNA double helix is reduced into single strands [59, 62].

In the next step, the temperature of the mixture decreased to a predetermined annealing temperature, usually between 50 and 60°C. In this step of PCR, the oligonucleotide primers can hybridise specifically to their complementary sequences, meaning that the primers can anneal to the DNA target sequence [59, 62].

Finally, the replication of the DNA strands occurs. After the annealing step, the temperature is raised to 72°C, and a DNA polymerase extends the primers by incorporating deoxynucleotides to form a new complementary strand of DNA [59, 62].

The cycle denaturation-annealing-extension is repeated over and over, usually 30 times, and new strands themselves as template for the DNA primers and the process lead to an exponential amplification of the DNA bounded by the primers [59, 61, 62]. These cycles allow an estimated enrichment of the selected sequence of 105 to 106 [61].

After the termination of the reaction cycles, the reaction products are separated by agarose gel electrophoresis, and finally they can be visualized directly by staining with ethidium bromide and examination of the gel under ultraviolet light [61].

An important aspect to take into consideration when analysing PCR results is that several parameters need to be controlled to obtain reliable quantitative expression measures. To this, it is often used an approach for the normalization of several parameters with an internal control gene. A gene valid to use as a reference gene requires an expression that do not vary in the tissues or cells under certain experimental conditions [48, 63]. One example of the most usually described normalization gene is glyceraldehyde-3-phosphate dehydrogenase (GAPDH). This gene is present in most cell types and it is considered a simple “housekeeping” protein that has been shown to be involved in many cellular processes in addition to glycolysis, where its function is catalysing the reversible oxidative phosphorylation of glyceraldeyade-3-phosphate [48, 63, 64].

2.4 - Nanomaterials in bone regeneration

Nanomaterials can be defined as the materials with dimensions less than 100 nm [1, 2, 65]. These materials include nanoparticles, nanoclusters, nanocrystals, nanotubes, nanofibres, nanowires, nanorods, nanofilms, etc. [2]

Nanomaterials are promising candidates in bone regeneration, since nanostructure provides a closer approximation to native bone architecture, compared to micron materials [2, 66].The decreasing material size leads to modification of the nanofeatured surfaces, increased surface area, surface roughness and surface to volume ratio, which creates superior physiochemical properties to the cellular behaviour [2, 66]. For example, increase of surface

energy and wettability, seen in nanostructured surfaces, allows to an increased protein adsorption and cell adhesion [66, 67].

Recently, more efforts are being made to repair and reconstruct bone damage using biomimetic bone tissue. To accomplish this, it is necessary to select biomaterials that are present in bone (e.g. HA and collagen), and it is also possible to incorporate growth factors (e.g. BMPs) and/or cells for bone repair and regeneration [66].

Based on the structure of the natural HA, nano-HA has been synthesized for various tissue engineering applications, such as for bone replacement and for the delivery of relevant drugs in the management of several bone diseases [68]. Furthermore, many studies revealed that biomimetic nano-HA enhances the proliferation and activity of bone cells in the regeneration process compared to the microstructured ceramic [67, 69-72]. *Webster et al. (2000)* showed that cell differentiation markers, such as alkaline phosphatase (ALP) synthesis and calcium deposition, were significantly greater on nanophase HA than on conventional ceramic [73].

2.4.1 - Hydroxyapatite

Bioceramics materials, namely calcium phosphate (CaP)-based materials, are widely used for bone regeneration and/or replacement in many biomedical applications. Synthetic HA is a CaP with the chemical formulae $Ca_{10}(PO_4)_6(OH)_2$, and a Ca/P ratio of 1.67, which is similar to the principal inorganic constituent of bone and teeth [3,5] . However, CaP can also exist with a Ca/P ratio lower than 1.67, referred as calcium-deficient hydroxyapatite (DHA), denoted by Ca_{10-x} $(HPO_4)_x(PO_4)_{6-x}(OH)_2$-x [5, 73, 74]. HA (Ca/P=1.67) has been extensively investigated because it is a thermodynamically stable CaP in the physical environment [3] and shows excellent biological characteristics, due to its natural biocompatibility and potential osteoconductive, osteoinductive, osteogenic and biodegradable properties [1, 69].

2.4.1.1 - Nanostructured and properties

HA is a polycrystalline CaP, with a definite crystallographic structure. The hexagonal crystalline structure of HA allows exact atomic positions, and this structure have a space group P63/m. This space is characterized by a six-fold c-axis perpendicular to three equivalent a-axes at 120° angles to each other. Calcium cations (Ca^{2+}) and phosphate anions (PO_4^{3-}) are arranged around columns of monovalent hydroxyl anions (OH^-) [3, 76, 77]. Figure 3 shows the unit of HA, composed by Ca, PO_4 and OH groups closely packed together. Also, it can be noted that PO_4 group provides the skeleton framework and gives the structure and its stability [78].

HA is a mineral with small nanosized dimensions and low crystallinity, properties that provide distinct features of the biological apatites. The synthetic HA can be synthesized using many processes. Crystallographic and chemical studies have confirmed that synthetic HA is similar to the natural HA found in bone and teeth [1, 77]. Therefore, the synthetic HA is widely used for bone regeneration and/or replacement in many biomedical applications.

Besides the similarities of the synthetic HA and natural HA, there are more advantages for its application in tissue engineering. Thus, synthetic HA shows biocompatibility, slow biodegradability in situ, and good osteoconductive and osteoinductive capabilities [1, 69, 79-81].

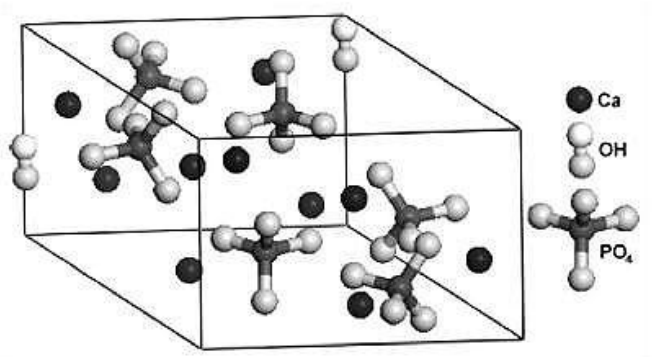

Figure 3 - Unit of hydroxyapatite hexagonally crystalline structure. *(Adopted from White et. al 2009).*

The nanophase HA powders show improved properties when compared with microphased powders, such as surface grain size, pore size and wettability, which may control protein interactions and thus guide cellular responses. Therefore, the nano-HA has a better bioactivity [3, 81], hence it allows a good osteoblast adhesion, proliferation, differentiation , osteointegration, and deposition of calcium-containing minerals on its surface, leading to an improvement of the composition of regenerated tissue within a short period [67,69-72,82].

In summary, according to the literature, nano-HA appears to have clear advantages in bone regeneration applications [83].

2.4.1.2 - Synthesis Methods

The nano-HA is an important material in bone regeneration, therefore there is a strong interest in its synthesis in an extra pure and well defined HA nanocrystals [20].

Several techniques have been developed to prepare nanosized HA, most of them involving wet and dry methods.

The dry methods for nano-HA synthesis are characterized by the preparation of the powder via application of high temperature, high-energy mechanical and controlled pressure. In this process, calcium and phosphorous compounds are used as reactants. These powders are mixed in acetone, calcinated in vacuum and, lastly, heat-treated with the supply of water vapour as the source of the hydroxyl group [1, 85]. The reactants used in the dry process can be several calcium and phosphorous compounds such as, dicalcium phosphate anhydrous ($CaHPO_4$), dicalcium phosphate dihydrate ($CaHPO_4.2H_2O$), monocalcium phosphate monohydrate ($Ca(H_2PO_4)_2.H_2O$) , calcium pyrophosphate ($Ca_2P_2O_7$), calcium carbonate ($CaCO_3$), calcium oxide (CaO) and calcium hydroxide ($Ca(OH)_2$), among others [85].

The wet chemical precipitation method (i.e. wet chemical precipitation, sol-gel, emulsion, biomimetics, among others) is widely used because it is significantly cheaper and easier than other methods of HA formation [1, 3, 74] and the probability of contamination during processing is very low [85]. Thus, this technique is more popular for synthesis nano-HA since, no specialized equipment is required and large quantities of material can be produced of nanostructured HA from aqueous solution [1, 3, 74].

The reaction of Yagai and Aoki (1) can be followed in order to obtain suspensions of HA nanoparticles. A solution of H_3PO_4 is dropped into a basic suspension of Ca $(OH)_2$ [1, 69, 86].

$$10Ca(OH)_2 + 6H_3PO_4 \rightarrow (Ca_{10}PO_4)_6OH_2 + 18H_2O \quad (1)$$

Other calcium compounds may be used to obtain suspensions of nanoparticles. For example, calcium nitrate tetrahydrate ($Ca(NO_3)_2.4H_2O$ can be added to ammonium dihydrogen phosphate ($NH_4H_2PO_4$)[1, 69].

In the wet chemical precipitation method, it is important that the reactants have the correct molar ratio of calcium and phosphorous and, also, to adjust and maintain the appropriate pH of the solution [87].

Synthesis of nano-HA by wet chemical precipitation allows controlling the particle shape, size and specific surface area, by monitoring the reactant addition rate, reaction temperature, pH, and the presence of additives [1, 69]. In literature, the crystallinity of HA is largely increases by reaction temperature [1, 69, 88].

2.4.1.3 - NETmix® Technology

The NETmix® is a novel technology (development at FEUP) that enables the production of nanomaterials, such as nano-HA, with a high reproducibility, mainly in terms of size distribution [4]. This technology is now being commercially applied by Fluidinova to the synthesis of highly pure hydroxyapatite nanoparticles, nanoXIM-HAp® [5, 15, 89].

The NETmix® is a patented static mixer, on continuous mode operation [89] for mixing of liquids and/or gases; it allows the control of fluid mixture in an optimized and reproducible way. [90] Furthermore, this technology shows reproducible and satisfactory results, especially with regard to distribution of particle sizes [91].

Its principal component is a network of chambers interconnected by channels, that is, the network combines, in an organized manner, chambers and channels [92]. This interconnection create zones that promote complete mixing and of complete segregation, as shown in figure 4 [5].

The implementation of the static mixer brought improvements in comparison with other static systems. For example, its structure is considerably simple; it allows the introduction of temperature, pressure and concentration sensors; it provides an easy implantation of different pre-mixing reactants injection schemes; it has the ability to control the mean residence time of the reactants and the mixing intensity and scale. Thus, this reactor is particularly suitable for reactions in which mixing quality and intensity are critical. [92]

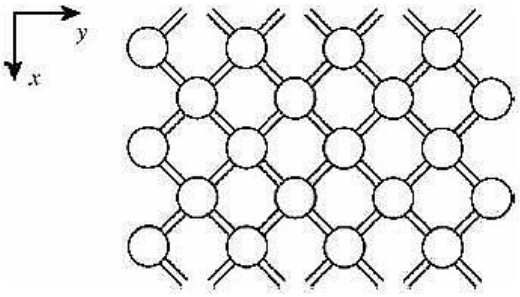

Figure 4 - Regular network of the reactor NETmix® in an association chambers and channels**.** *(Adopted from Silva et. al 2008).*

The NETmix® regulates micromixing; this phenomenon is associated to the homogenization of the mixture at the smallest scale [92, 93]. The properties of the HA produced by NETmix®, such as purity, crystallinity, particle size distribution, crystallites size and morphology, can be determine by the micromixing characteristics [74].

In the laboratory, the prototype of this technology, consisting of a network of spherical chambers and cylindrical channels, was developed and used for the synthesis of nano-HA with high reproducibility, mainly in terms of size distribution [5]. The NETmix® reactor, for the synthesis of nano-HA, is based on the wet chemical precipitation method at room temperature [89].

Therefore, to produce nano-HA is necessary to feed the reactor with a calcium solution, a phosphorous solution and an alkaline solution and, optionally, one solvent or dispersing agent [74]. The initial reactants are injected in inlet chambers through the back and front feeding channels (figure 5).

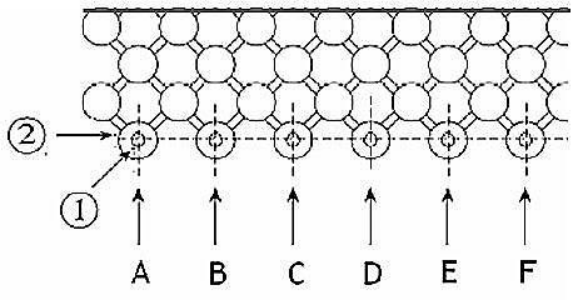

Figure 5 - Representation of the feed system NETmix® reactor. (1) Feeding channels; (2) inlet chambers; (A-F) reagents inlet. *(Adopted from Faria et. al 2008).*

The products synthesized by this technology can be collected in the form of suspension at the exit or the intermediate position of the reactor. Then, the suspension can be subjected to a separation process in order to concentrate the particles. Moreover, the concentrated particles can be washed for the elimination of the supernatant, and they can be exposed to drying processes. Thereafter, the particles may be subjected to several stages of grinding and thermal treatments. [89]

From its versatile technology, NETmix® Fluidinova is responsible by launching several products with a single phase and high purity, such as the nanoXIM•HAp102®. This product is a highly pure nanocrystalline hydroxyapatite in paste form at 15% (weight/volume) nano-HA concentration in pure water.

In summary, the NETmix® technology results from the application of a novel concept for producing HA nanoparticles, based on wet chemical precipitation method at room temperature. This patented industrial process is able of controlling, at the molecular level, the calcium and phosphate reaction to produce HA nanoparticles [6, 74, 94].

2.4.1.4 - Applications

Synthetic nanosized HA is the most stable CaP and it has been used for a variety of biomedical applications, such as in dentistry, matrices for drug release control and surgery for hard tissue repair [1, 3, 77, 95]. The previous studies have been so far mostly used owing to its chemical similarity to the mineral component of calcified tissue [3, 5, 95]. In addition, other properties have attracted interest, such as their high surface area, their ability to become dispersed in aqueous solutions and their higher reactivity and adsorption, over the same material of micrometric size [2].

Nano-HA is a bioactive ceramic that has been preferred for hard tissue repair and as coatings for metal prosthesis over autografts and allografts. For some time now, it appears

that synthetic HA increases the response regarding bone bonding. Accordingly, the nano-HA is used as an implant coating to stimulate bone growth around the implant. [3, 96]

Many studies have demonstrated that the mechanical strength and fracture toughness of HA can be improved by the use of nanoscale powders; the large surface area to volume ratios of the particles contributed for a better densification [76]. Accordingly, nano-HA can be used to produce scaffolds for tissue engineering, and when nano-HA is compressed, for example into a cylinder, it has attracted interest for bone replacement [3, 97].

The nano-HA particles with high surface area and un-agglomerated are of interest for injectable or controlled setting bone cements, high strength porous or non-porous synthetic bone grafts and the reinforcing phase in nanocomposites that attempt to mimic the complex structure and superior mechanical proprieties of bone [98]. Furthermore, the nano-HA has been widely used in dentistry. *Huang et al.*, [99] for example, showed that nano-HA had the potential to remineralize initial enamel caries lesions.

Recently, many researchers have interest in using the magnetic nano-HA, since it is possible to couple HA with magnetic particles such as cobalt (Co), iron (Fe) and magnetite (Fe_3O_4) [3, 77]. This magnetic coupling aims at particle delivery by external control of a magnetic field. The magnetic HA composites are adapted for biological applications such as cell separation, drug delivery, contrast agents for magnetic resonance imaging (MRI), and heat mediators for hyperthermia [3, 100]. Moreover, other studies suggested that nano-HA coated magnetic particles could be used to reverse osteoporosis [101-103], once osteoblast density and osteoblast differentiation markers are significantly increased in the present HA-coated-Fe_3O_4 [102].

2.5 - Interactions cells – Nanostructured materials

Nanostructured materials for bone applications have the ability to improve surface reactivity, because surface area-to-volume ratios increase with decreasing particle size [1, 104]. According to literature, the surface properties (such as surface area, charge, and topography) are related to the grain size of a material, thus the cell response to the nanoparticles is significantly different that the one observed during the cell interaction with the bulk materials [66, 68, 104, 105].

In particular, for cell interaction it is beneficial if the surface roughness of HA is in the nanoscale range but the reasons for this improvement are not completely understood. [3] However, it is believed that protein adsorption and bioactivity on particles with nanometer features is different from that on conventional materials. Interaction between cells and nanostructured materials also depends on receptors on the cell surface and the protein layer adsorbed onto the material surface [3]. It is reported that the adsorption and conformation (or bioactivity) of proteins that mediate specific osteoblast adhesion (such as fibronectin and vitronectin) are enhanced on nanophase material [67, 84, 73].

Several studies on the cell response to HA nanoparticles have shown that HA particles are internalized through endocytosis, and the cell response appears to depend on the combined interaction of multiple nanoparticles characteristics [5, 68, 106-108]. An important aspect in the modulation of the cell behaviour is that the HA nanoparticles may be digested in the lysosomes, leading to an increase of the levels of Ca^{2+} in the cytoplasm. Suitable concentration of Ca^{2+} is favourable for the proliferation and osteoblast differentiation [109].

2.5.1 - Apoptosis

Investigation of the cell-material interaction is mainly focused on biocompatibility. However, nowadays much attention is given to the possibility of apoptosis induced by biomaterial, once apoptosis could be caused by inducing factors, and many disease therapies are closely related to inducing apoptosis.

Apoptosis is recognized by an important mode of programmed cell death, which involves the genetically determined elimination of cells. It is a homeostatic mechanism responsible for the maintenance of normal cellular homeostasis [110, 111]. Moreover, this process can occur as a defence mechanism against cellular damage caused by disease or noxious agents. [110, 111] In other words, this phenomenon can be activated or inhibited by several stimuli, both physiological and pathological [111].

It is important to note that there are other forms of cell death, such as, necrosis, and other forms may be discovered. Moreover, there are cells that die with atypical characteristics, which are not categorized as apoptosis or necrosis [112].

Apoptosis contrasted with necrosis. Necrosis is considered to be a toxic process characterized by loss of cell membrane integrity leading to the release of the cytoplasmic contents, which causes the recruitment of inflammatory cells. Once apoptotic cells do not release the cytoplasmic contents and apoptotic cells or cell fragments are quickly phagocytized they have a little or no immune response [112].

Apoptosis can be considered a coordinated and often energy dependent process that involves caspase activity, DNA fragmentation and a complete cascade of events [110, 1110, 113].

Caspases are a family of cysteine aspartate-specific proteases that have a critical role in biochemical events associated with apoptosis [114, 115]. In particular, the activation of caspase-3 protease has been described as an “effector” caspase associated with the initiation of the “death cascade” and is therefore an important marker of the cells when they are into apoptotic signalling pathway [116].

Nowadays, there are many methods to determine apoptosis in cells through the evaluation of the activity of proteins involved in apoptosis. Note that when there is the activation of caspase-3 there is substrate specificity for the amino sequence aspartate-glutamate-valine-aspartate. Thereby, the substrate can be used to continuously monitor the activity of caspase-3. Upon enzymatic cleavage, the nonfluorescent substrate is converted in a two-step process to a fluorescent compound. So, this is the base for caspase-3 activity assay that detect apoptotic events [110,112]. This assay requires cell lysis, which aims to release the enzyme into solution, followed by detection with a fluorescent labelled substrate with the appropriate excitation and emission settings [110,112]. Detection of caspases represents a rapid and consistent method for quantification of apoptotic cells [110,112].

Another form to analyse cell apoptosis is through morphological characteristics observation of the cells by standard transmission electron microscopy (TEM). This technique allows to define characteristics of an apoptotic cell, such as intact cellular membranes, dark and dense cytoplasm and nucleus, blebs at the cell surface, large clear vacuoles, disorganized cytoplasmic organization and nuclear fragmentation [110-112]. Thereby, TEM is used to confirm apoptosis once the categorization of apoptotic cells is irrefutable in case the cell contains certain morphological characteristics of an apoptotic cell [111, 112].

Chapter 3

Materials and Methods

3.1 - NanoXIM•HAp102®

NanoXIM•HAp102® is a new nanoparticle formulation which is provided by Fluidinova, Engenharia de Fluídos S.A. It was obtained by NETmix® technology. This synthetic product is a highly pure nanocrystalline HA in past form at 15% (weight/volume) in pure water. This paste is formed by nanocrystals of HA with an aspect ratio of 1:10 (Annex 1), and a size typically less than 100 nm, as determined by high resolution transmission electron microscopy (TEM). This synthetic hydroxyapatite has a stoichiometric ratio of Ca/P=1.67±1%.

The NanoXIM•HAp102® is characterized as having a single hydroxyapatite phase. This is a particularly relevant characteristic of the quality of nanoXIM•HAp products, verified for calcination temperatures of 1000ºC.

The above information of NanoXIM•HAp102® was obtained from the technical datasheet supplied by Fluidinova, which is presented in Annex 1.

Prior to the biological experiments, HA past was subjected to sterilization by gamma radiation.

3.2 - Pre-test: dose-dependent effect of nano-HA in MG63 osteoblast-like cells

A preliminary experiment was performed in order to select the appropriate concentration range of nano-HA to be tested in mesenchymal stem cells. The MG63 osteoblast-like cell line was used in this experiment.

MG63 cells were cultured in α-minimal essential medium (α-MEM) (31885-049, Gibco-Invitrogen) supplemented with 10% (v/v) fetal bovine serum (FBS-MSC Expansion ref. 12662-029, Gibco-Invitrogen), 1% (v/v) Penicillin/Streptomycin (15140-122, Alfagene), 1% (v/v) fungizone (15140-122, Alfagene) and 50 μg/mL ascorbic acid (15140-122, Alfagene), and were maintained in a humidified atmosphere with 5% CO_2 at 37°C. For subculture, the cell monolayer was washed twice with phosphate-buffered saline (PBS) and incubated with trypsin–EDTA solution (0.05% trypsin, 0.25% EDTA) for 10 min at 37°C to detach the cells.

Then, complete culture medium (2x the volume of trypsin that was used) was added to stop the reaction. Cells were re-suspended in culture medium and were seeded at density of 10^4 cells/cm^2 in 96-well plates. After 24h, the culture medium was removed and replaced by one containing nano-HA. The following concentrations were tested: 1, 10, 50, 100, 500 and 1000 µg/mL. Cultures were maintained for 2, 4 and 7 days, without any medium change. Cultures grown in the absence of nano-HA were used as control. This pre-test was conducted with four replicates. Dose-effects of nano-HA in MG63 cells were evaluated by the MTT assay, as it is described below.

3.3 - Culture of hMSCs

hMSCs (P10576, Lonza) were routinely cultured in α-minimal essential medium (α-MEM) (31885-049, Gibco-Invitrogen) supplemented with 10% (v/v) foetal bovine serum (FBS-MSC Expansion ref. 12662-029, Gibco-Invitrogen), 1% (v/v) Penicillin/Streptomycin (15140-122, Alfagene), 1% (v/v) fungizone (15140-122, Alfagene) and 50 µg/mL (v/v) ascorbic acid (15140-122, Alfagene). Cells were seeded in 90 mm diameter culture plates and were maintained in a humidified atmosphere with 5% CO_2 at 37°C. When the cells had grown to confluence, they were washed three times with sterile PBS, and adherent cells were detached by adding 1mL of trypsin (solution of 0.04% trypsin in 0.25% EDTA 25200-056, Gibbo, Invitrogen); cells were kept in an incubator (37°C and 5% CO_2) for 10 minutes to detach the cells. Then, complete culture medium (2x the volume of trypsin that was used) was added to stop the reaction.

To analyse the effect of nano-HA on the behaviour of hMSCs, 10^4 cells/cm^2 were seeded in 96-well and 6-well plates. At the 6^{th} day, nano-HA was added to the cultures. Nano-HA was tested at the following concentrations: 1, 10, 50 and 100 µg/mL. Cultures performed in the absence of nano-HA were used as control. Cultures were maintained for 21 days, and the culture medium (which did not contain nano-HA) was changed twice a week. Cultures were characterized at days 7, 14 and 21, as described below.

3.4 - Characterization of the cell cultures

3.4.1 - Metabolic activity/cell proliferation

Metabolic activity of hMSCs was evaluated at 3, 6, 7, 14 and 21 days by the MTT assay. In this assay, the MTT 3-(4,5-dimethylthiazol-2-yl)-2,5-diphenyl tetrazolium bromide (MTT; Sigma M2128) is reduced to a formazan product by active mitochondrial dehydrogenases of living cells. MTT assay was also performed in wells containing the culture medium with the nano-HA (without cells), to be used as "blanks", to correct for the eventual interferences of nano-HA with the MTT assay. Briefly, for the assay, cells seeded on 96-well plates were incubated with MTT (0.5 mg/mL), for 3h to allow the formation of formazan crystals. After this period, the supernatant was discarded and 150 µl dimethyl sulphoxide (DMSO) (131954.1611 1 L, Panreac) was added to dissolve the purple formazan crystals. Then, 100 µL of the supernatant were transferred to a RIA plate (96-well plate) and the absorbance was read at 550 nm in an ELISA reader (BioTek synergy HT). Results were expressed as absorbance values.

3.4.2 - Cell morphology and F-actin cytoskeletal organization

Cytoskeletal organization was followed by F-actin/DNA staining. Cultures were rinsed with PBS at 37ºC and were fixed in 3.7% paraformaldehyde (PFA) for 15 minutes at the room temperature; PFA was removed and cultures were rinsed twice with PBS. Subsequently, cells were permeabilized in 0.2% (V/V) Triton X-100 (Sigma T-8787) in PBS, for 10 minutes at room temperature, and then rinsed 3 times with PBS. After, cultures were incubated with 1% (V/V) BSA solution in PBS for 1h at room temperature. Following, the samples were incubated with Alexa Fluor 488 phalloidin (Molecular Probes A-12379) diluted 1:40 in the BSA/PBS solution, for 1h in the dark at room temperature, for the staining of the F-actin filaments. After, the samples were washed 3 times with PBS. Cell nuclei were counterstained with propidium iodide (P4170-10MG Sigma) diluted 1:10000 in PBS. The samples were incubated with propidium iodide solution for 10 minutes at room temperature. The propidium iodide was removed washed 3 times with PBS. Finally, samples were covered with Fluoromount™ Aqueous Mounting Medium (F4680; Sigma) and remained at 4ºC in the dark until observation. Samples were observed by Confocal Laser Scanning Microscopy (CLSM) at days 7, 14 and 21 of culture. Images were acquired on a Leica TCP SP2 AOBS microscope.

3.4.3 - Alkaline phosphatase and collagen histochemical staining

At days 7, 14 and 21 the presence of ALP and collagen in cell cultures was visualized by histochemical staining. Cultures were rinsed with PBS at 37ºC and fixed with 1.5% glutaraldehyde in 0.14 M sodium cacodylate buffer for 10 min. For ALP staining, cultures were incubated in a diluted alkaline solution of Na-α-naphthyl phosphate substrate (N7255-1G, Sigma) in tris buffer 0.1 M pH 10 (T-8524, Sigma) containing the Fast Violet RR salt (F-0500, Sigma), for 1h in the dark. After staining, the samples were rinsed with water to remove the excess of dye. Cells containing ALP on their surface developed a brown to black stain after the incubation period.

For collagen histochemical staining, fixed samples were washed with PBS and left to dry in the air. Dried samples were incubated with dye sirius red for 1h at room temperature. This dye was prepared in picric acid at a concentration of 100 mg/100 ml. Then, the dye was discarded and samples were washed four times with hydrochloric acid 0.01 M to remove the excess of dye. Collagen stained red after the incubation period.

After staining, both samples were observed in a Nikon TMS optical microscope and images were captured using Eclipse Net software.

3.4.5 - Transmission electron microscopy (TEM)

Cultures were observed by transmission electron microscopy (TEM) at days 7, 14 and 21, for assessment of morphology characteristics and nano-HA uptake. For this, cultures were washed three times with PBS at 37ºC. Then, adherent cells were enzymatically released (0.05% trypsin, 0.25% EDTA; 4 minutes) and the cell suspensions were centrifuged at 5000 rpm for 10 min. The resulting pellet was fixed in 2.5 % glutaraldehyde for 2h at 4ºC, post fixed with 2 % osmium tetroxide, dehydrated in graded ethanol and later embedded in Epon, using routine methods. Ultra-thin (100 nm) sections mounted in copper grids (300 Mesh) were contrasted with uranyl acetate and lead citrate for TEM analysis (ZeissEM10A) at an accelerating voltage 60 kV.

3.4.6 - Scanning Electron Microscope (SEM)

Scanning Electron Microscopy (SEM) was used to analyse the cell morphology and the organization of the cell layer.

Cultures were washed with PBS at 37ºC and they were fixed in 1.5 %(v/v) glutaraldehyde in 0.1 M sodium cacodylate solution at RT for 10 min. Fixed samples were washed with PBS and stored in cacodilate buffer at 4ºC. Before SEM observation, the fixed samples were dried with increasing concentration of alcohols (70, 80, 2 x 90 and 99.8 % v/v), critical-point dried and sputter-coated with gold (80%) and palladium (20%) alloy under high vacuum. The samples were analyzed in a JeoL JSM 6301F scanning electron microscope equipped with an X-ray energy dispersive spectroscopy (EDX) microanalysis capability (Voyager XRMA System, Noran Instruments).

3.4.7 - Apoptosis

Apoptosis was assessed by EnzCk®Caspase-3 assay kit (Molecular Probes) on days 7, 14 and 21 of culture. The programmed cell death was detected from cell cultures using this kit according to manufacturer's instructions. This technique allows detection of apoptosis by assaying for the increase in caspases-3. Initially, cells were washed twice with PBS and then lysed with 0.1% (V/V) Triton X-100 for 15 minutes. The supernatants from each sample were transferred to 96-well plate black and assayed for caspase-3 activity. The fluorescence was measured using an ELISA reader (BioTek synergy HT) with excitation at 485 nm and emission at 528 nm. Results were expressed as the amount of fluorescence.

3.4.8 - Gene expression by reverse-transcription polymerase chain reaction (RT-PCR)

Cell cultures were assessed on days 7, 14 and 21 by RT-PCR for the expression of the housekeeping gene GAPDH and the osteoblastic genes RUNX 2, Col I, ALP, OPG and BMP-2. Total RNA was extracted from cell cultures using NucleoSpin®RNA kit according to manufacturer's instructions. RNA was quantified by measuring the absorbance of the samples at 260 nm. RT reaction mixtures consisted of extracted RNA, RT-PCR buffer, dithiothreitol (dTT), deoxynucleoside triphosphate (dNTPs), primers sequence forward (PF) and reverse (PR) for each gene tested, Taq-DNA polymerase and water in a final volume of 25 µL. The complementary DNAs (cDNAs) were then amplified with recombinant Taq-DNA polymerase with the Titan One Tube RT-PCR System (Roche) under the following conditions: 30 cycles of denaturation (94ºC/30 s), annealing with specific temperature for each gene tested (table I), elongation (68ºC/45 s), and followed by a prolonged elongation of 7 min at 68ºC. Table I shows the primers sequences and annealing temperatures that were used for PCR amplification. The RT-PCR products were electrophoresed on 1% (weight/volume) agarose gel and stained with ethidium bromide. The gel pictures were taken with a camera under ultraviolet illumination. The area and integrated density (ID) of bands were calculated with ImageJ 1.41 software. The ID values obtained were normalized to the corresponding ID value of GADPH that served as the internal control.

Table.1 - Primers for RT-PCR amplification and optimal annealing temperature

Gene	5´Primer	3´Primer	Annealing T(°C)
GAPDH	5´-CAGGACCAGGTTCACCAACAAGT-3´	5´-GTGGCAGTGATGGCATGGACTGT-3´	55
RUNX 2	5'-CAGTTCCCAAGCATTTCATCC-3'	5'-TCAATATGGTCGCCAAACAG-3'	55
Col I	5´-TCCGGCTCCTGCTCCTCTTA-3´	5´-ACCAGCAGGACCAGCATCTC-3´	55
ALP	5´-ACGTGGCTAAGAATGTCATC-3´	5´-CTGGTAGGCGATGTCCTTA-3´	55
OPG	5'-AAGGAGCTGCAGTACGTCAA-3'	5'-CTGCTCGAAGGTGAGGTTAG-3'	60
BMP-2	5´-GCAATGGCCTTATCTGTGAC-3´	5´-GCAATGGCCTTATCTGTGAC-3´	60

3.5. Statistical analysis

Results are presented as mean ± standard deviation. Three independent experiments were performed. In each experiment, four replicas were set up for the biochemical assays and two replicas for the qualitative assays. Statistical differences between control cultures and cultures exposed to nano-HA were determined with the non-parametric tests unpaired t tests. Differences between groups were considered statistically different for p-values less than 0.05 ($p < 0.05$). Calculations were performed using GraphPad Prism software for Windows (version 5.0).

Chapter 4

Results

4.1 - Pre-test: dose-dependent effect of nano-HA in MG63 osteoblast-like cells

Initially, the dose-dependent effects of nano-HA were investigated in MG63 cells cultured for 7 days in the presence of nano-HA in the concentration range 1-1000 μg/mL, by evaluating the metabolic activity/cell proliferation by the MTT assay. Results are presented in figure 6.

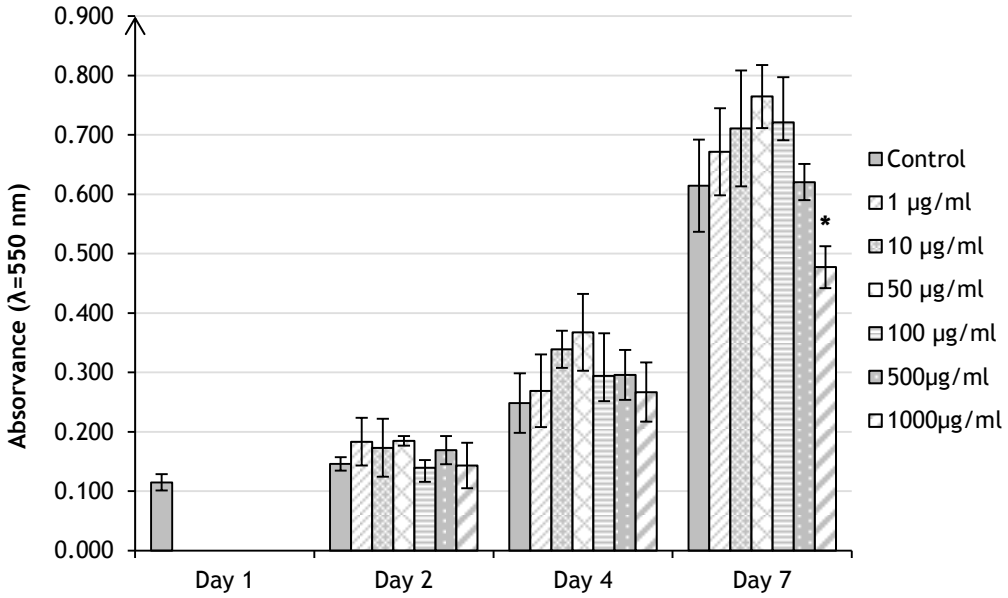

Figure 6 - Metabolic activity/cell proliferation profile of MG63 osteoblast-like cells cultured in the presence of different nano-HA concentrations, at days 2, 4 and 7. Nano-HA was added 24h after cell seeding. Cell metabolic activity was determined using the MTT assay. The in absence of nano-HA were used as control. Results of MTT assays were expressed as means ± standard deviation (SD). Asterisks (*) indicate a significant difference ($p < 0.05$) from control (absence of nano-HA).

In control conditions, values for the MTT reduction increased during the 7-day culture period. The presence of nano-HA tended to cause an increase at day 4 (10 and 50 μg/mL) and at day 7 (1 to 100 μg/mL), but this increase did not attain statistical significance. However, at the concentration of 1000 μg/mL the metabolic activity/cell proliferation was significantly lower than in control at day 7.

With this information, the effect of nano-HA in hMSCs was tested for the concentrations 1, 10, 50 and 100 μg/mL. The response of hMSCs to nano-HA was characterized for cell viability/proliferation, DNA quantification, histochemical staining of ALP and collagen, apoptosis and expression of osteoblastic genes. In addition, cultures were observed by SEM, CLSM and TEM.

4.2 - Behaviour of hMSCs in the presence of nano-HA

4.2.1 - Metabolic activity/cell proliferation

Cell viability/proliferation of hMSCs exposed to nano-HA on different conditions of culture was measured by the MTT assay. Results are presented in figure 7. In control conditions (absence of nano-HA) cell viability/proliferation increased during the 21-day culture time. Nano-HA was added at day 6, and cultures were assessed at days 7, 14 and 21. At day 7 (1 day after the addition of nano-HA), there was a tendency for an increase in the presence of 50 and 100 μg/mL, but this effect did not attain statistical significance. At day 14 (7 days after the addition of nano-HA), a dose-dependent decrease was observed, with a statistical significant value in the presence of 100 μg/mL nano-HA. However, cultures exposed to the lower nano-HA levels were able to recover from this deleterious effect and, at day 21, significantly increased values were measured in the cultures exposed to 10 μg/mL. Still, exposure to higher levels of nano-HA (50 and 100 μg/mL) cause a decrease in the cell viability/proliferation (~38 and 29%).

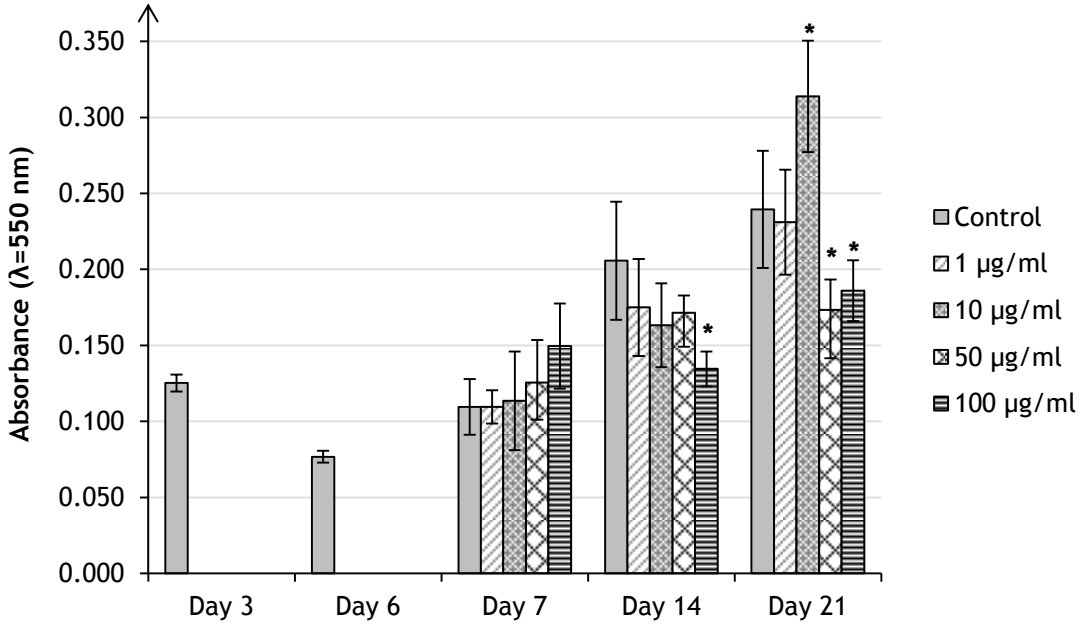

Figure 7 - Metabolic activity/cell proliferation profile of hMSCs cultured in the presence of different nano-HA concentrations at days 7, 14 and 21, assessed by the MTT assay. Nano-HA was added at day 6 Results were expressed as means ± standard deviation (SD). Asterisks (*) indicate a significant difference ($p < 0.05$) from control (absence of nano-HA).

4.2.2 - Alkaline phosphatase and collagen histochemical staining

Control cultures and cultures exposed to 10 and 50 µg/mL were stained for the presence of ALP and collagen, at days 7, 14 and 21 Figure 8 shows a low magnification image (x2) of the stained cultures, which allows a better perception for how to hMSCs behaved throughout the 21-day culture time. Both control and nano-HA-exposed cultures presented cell clusters which increased in size and staining intensity from day 7 to day 21. Compared to control, cultures performed in the presence of 10 µg/mL nano-HA showed higher ALP staining at days 14 and 21 and higher collagen staining at day 21. However, nano-HA, at 50 µg/mL, caused a deleterious effect, evident at day 21, as suggested by the presence of small sized cell clusters exhibiting low staining intensity.

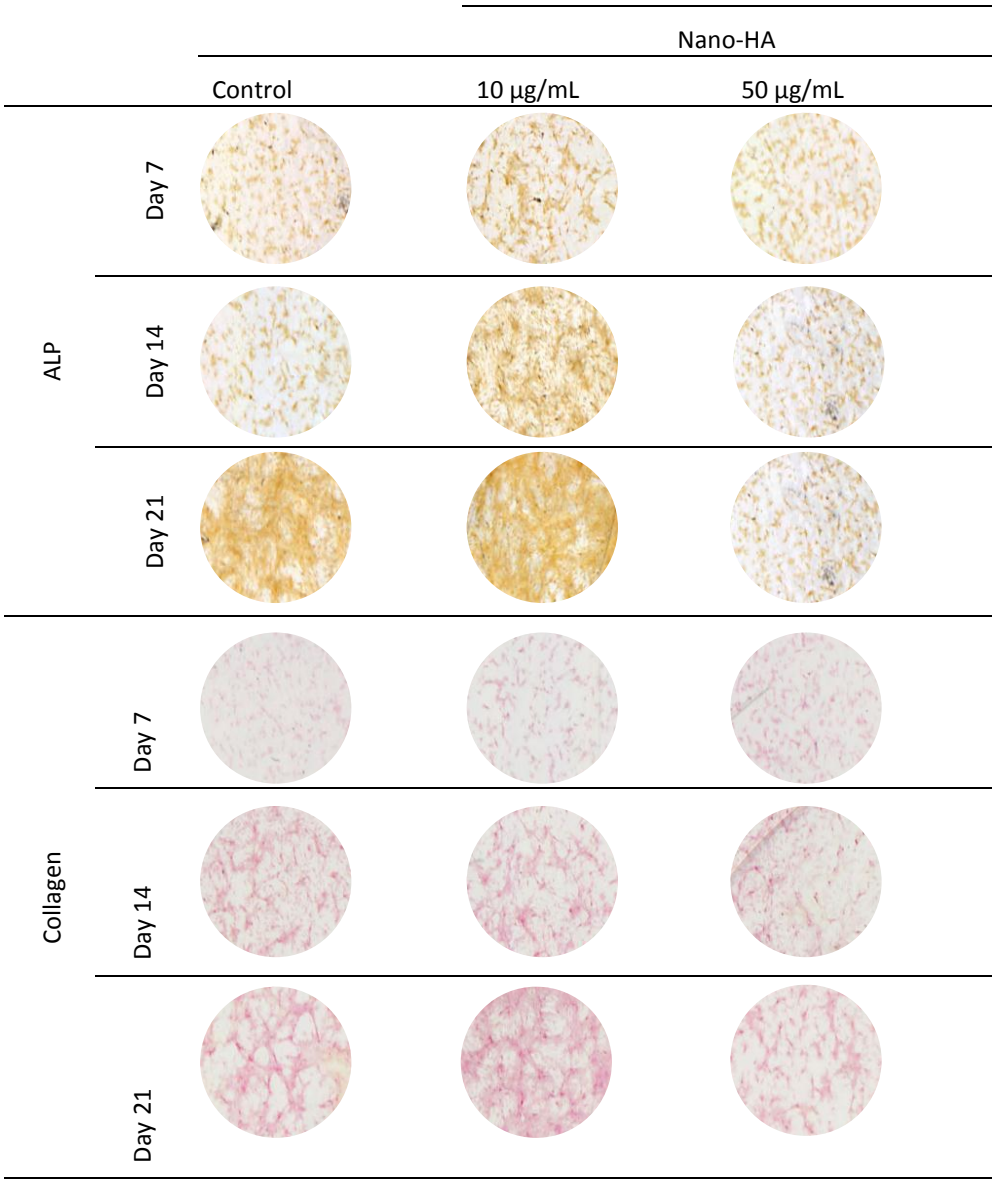

Figure 8 - Low magnification view of hMSCs cultured in the absence (control) and in the presence of 10 and 50 µg/mL nano-HA, stained for ALP and Collagen, at days 7, 14 and 21. ALP is shown by a brown to black stain, and collagen by a red stain. Magnification: 2X.

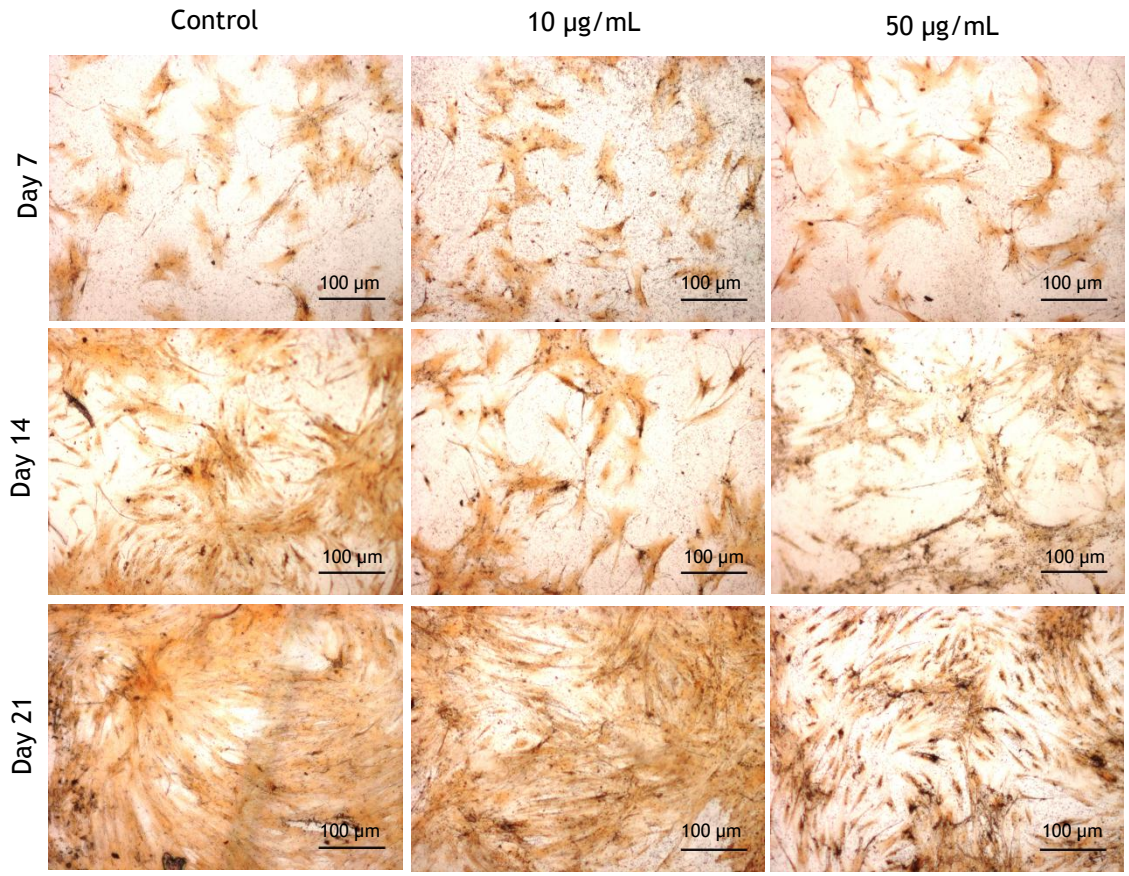

Figure 9 - Images of ALP histochemical staining of hMSCs cultured in the absence (control) and in the presence of 10 and 50 µg/mL nano-HA, at days 7, 14 and 21. The presence of ALP is shown by a brown to black stain. Magnification: 200 X. Scale bar = 100 µm

Figures 9 and 10 present microscopic images of the cultures stained for ALP and collagen, respectively. Histochemical staining increased from day 7 to day 21. Cultures showed a typical pattern of cell growth with the presence of cell clusters showing areas of higher cell density giving a nodular appearance. These cell clusters stained intensively for ALP and collagen. The presence of 10 µg/mL nano-HA caused an increase in the staining intensity at day 21. Exposure to 50 µg/mL nano-HA resulted in some loss of the typical pattern of cell growth and, apparently, a lower number of adherent cells.

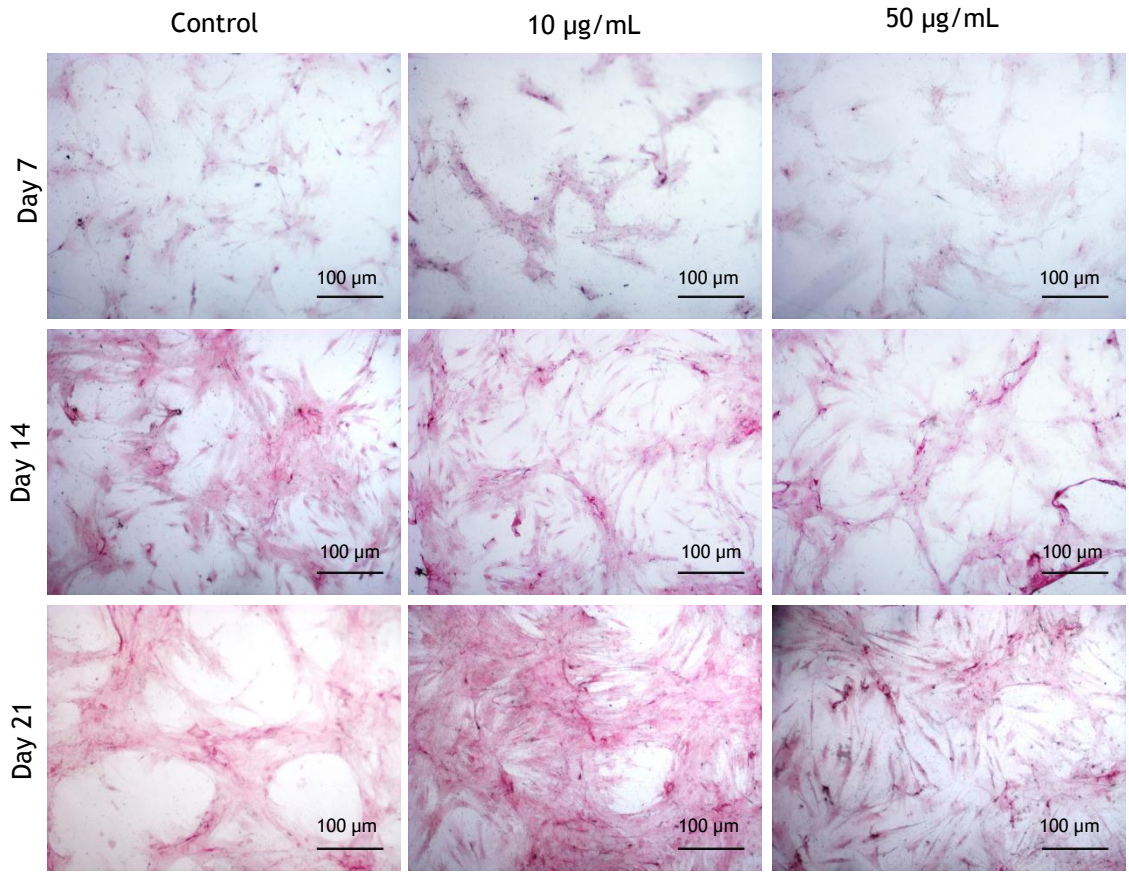

Figure 10 - Images of Collagen histochemical staining of hMSCs cultured in the absence (control) and in the presence of 10 and 50 µg/mL nano-HA, at days 7, 14 and 21The presence of collagen is shown by red to pink stain. Magnification: 200X.

4.2.3 - Scanning Electron Microscope (SEM)

On SEM observation, figure 11, hMSCs presented a spread appearance with an elongated/polygonal morphology, both in control cultures and in the presence of nano-HA (10 and 50 µg/mL). Cells exhibit long cytoplasmic projections (filopodia) and cell-to-cell interactions. In addition, the cell layer increased along the culture time. When the cultures exposed to nano-HA, the HA particles appeared to be closely associated with the cell layer, suggesting a high affinity between the cells and the HA particles. High magnification SEM images, figure 12, shows a detailed view of this interaction. Nano-HA particles appeared as different sized agglomerates that appeared to be located over the cell surface and also inside the cell. Figure 13A also illustrate this behaviour, showing agglomerates that are placed on the cell surface (marked as +) but others that seemed to have a intracellular location (marked with an *).

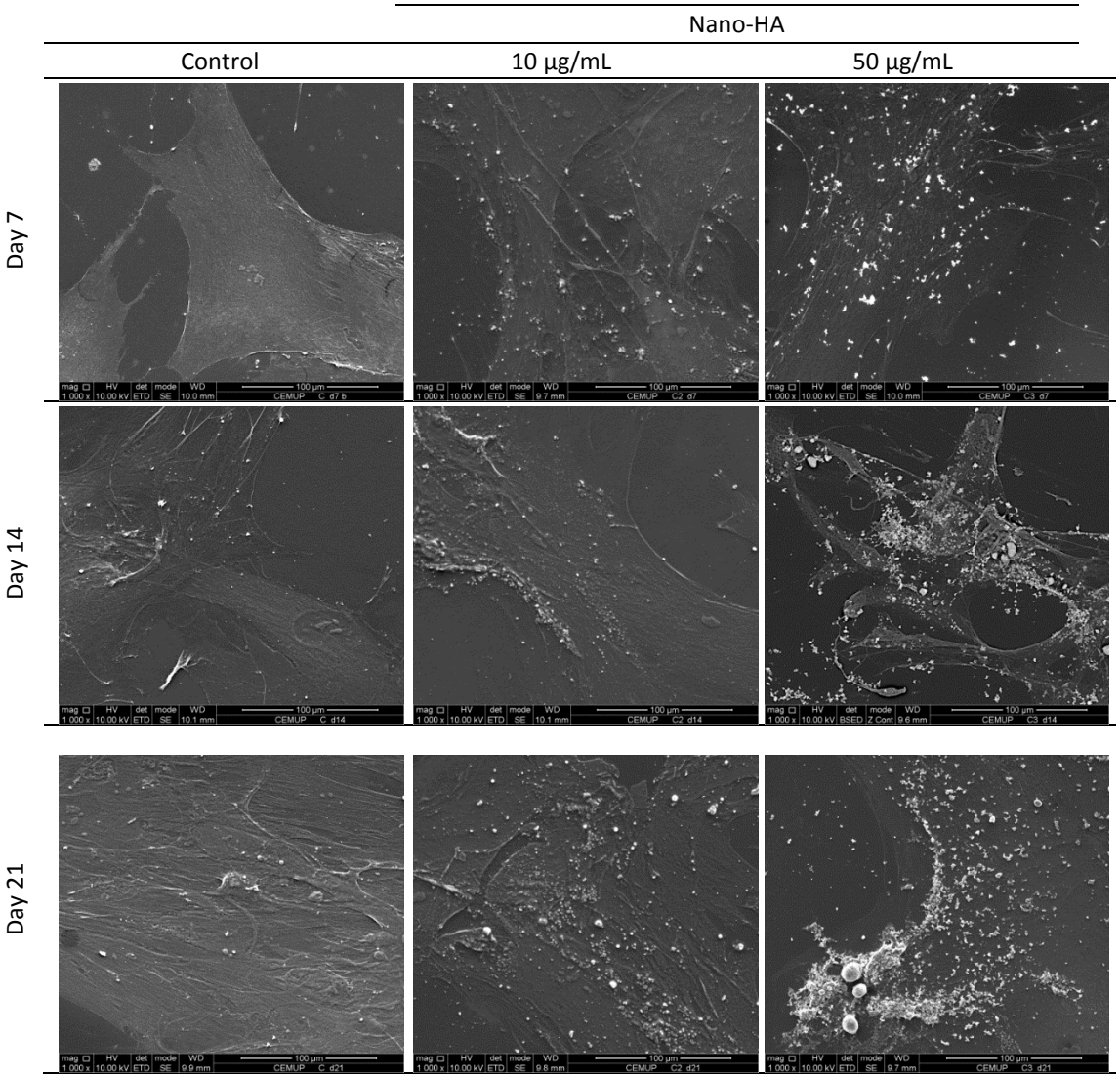

Figure 11 - SEM images of hMSCs cultured in the absence (control) and in the presence of 10 and 50 µg/mL nano-HA, at days 7, 14 and 21. Magnifications: 1000x.

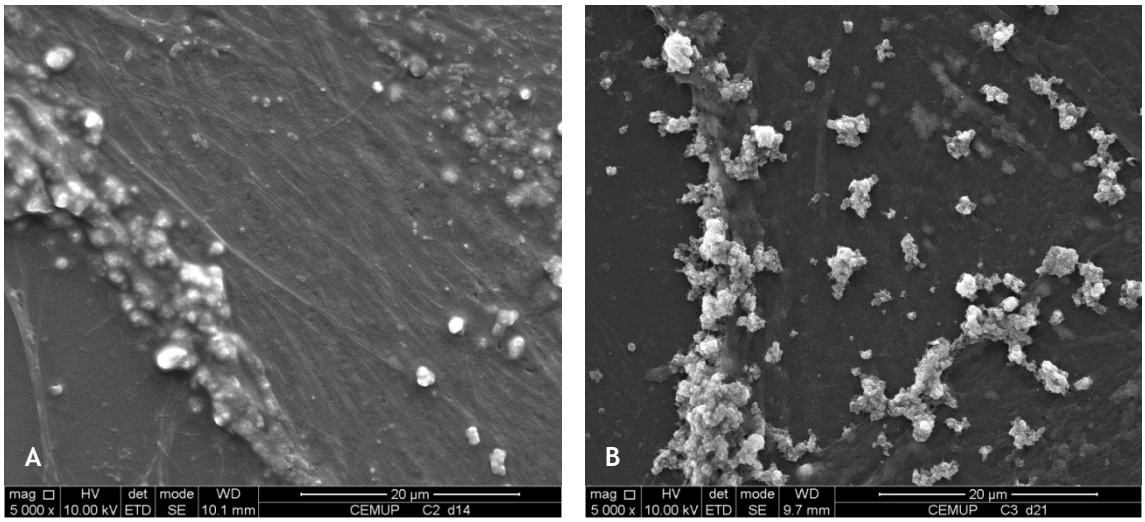

Figure 12 - High magnification SEM images of hMSCs cultured in the presence of nano-HA. (A) Cultures exposed to 10 µg/mL, 14 days; (B) cultures exposed to 50 µg/mL, 21 days. Magnification: 5 000 x.

EDS analysis was performed in order to confirm the elemental composition of the nano-HA agglomerates. Figure 13 **(right side).** shows the EDS spectra of the particles that were seen in the culture substrate (#) and that appeared to be present inside the cell (*), respectively Z1 and Z3 spectra, indicating that particle's aggregates contain of calcium, phosphorus and oxygen, evidencing the presence of a calcium phosphate compound. The Z2 spectrum shows only the peak of the carbon which it is characteristic of the culture substrate. The spectrum Z2 was determined in order to confirm that the main elements detected in the Z1 and Z3 spectrum are not derived from the culture substrate. Figure 13B displays a high magnification SEM image of a nano-HA micro agglomerate, showing the individual nanoparticles.

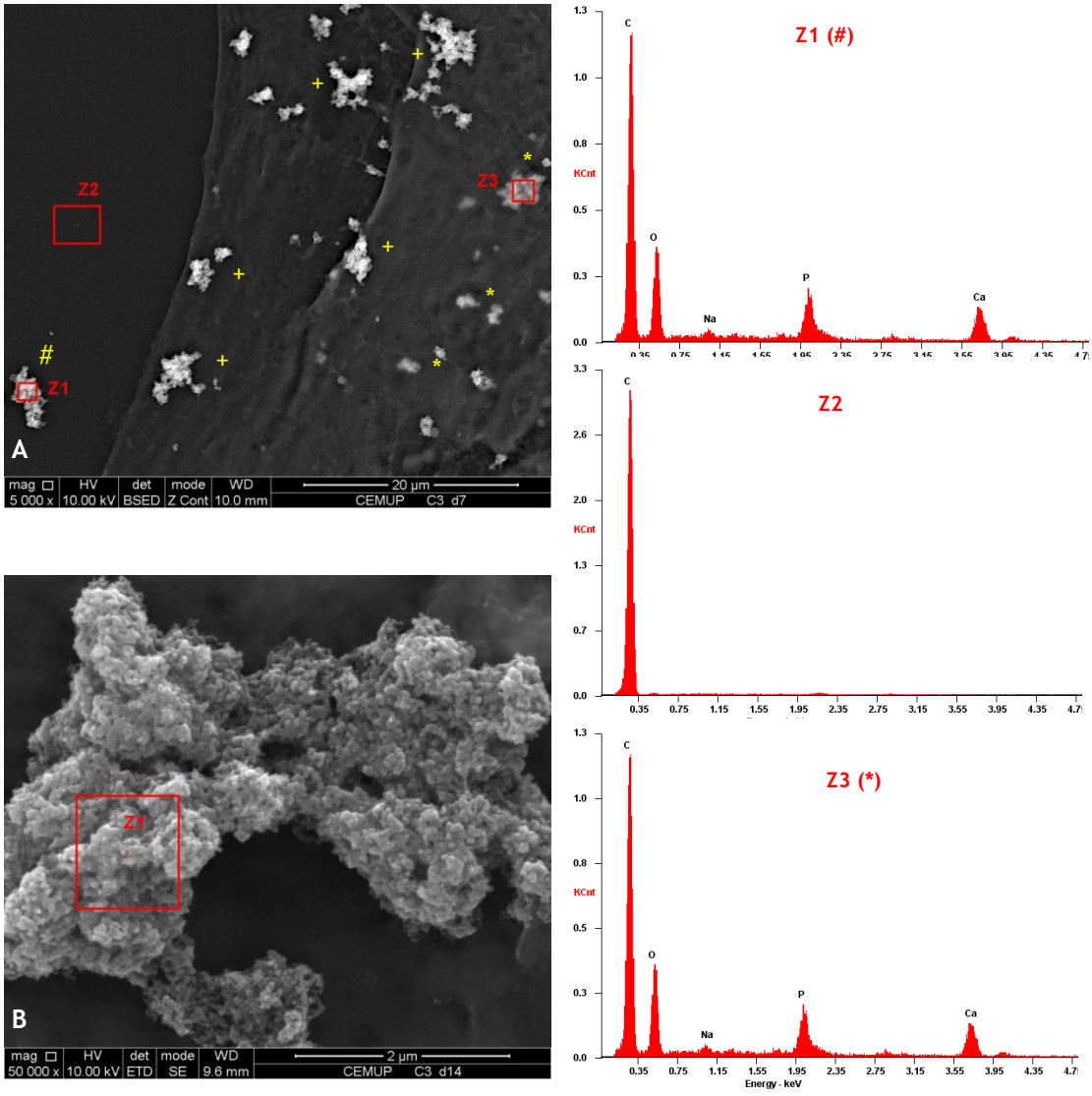

Figure 13 - SEM images (left side) and EDS spectra of selected areas (right side). A: detailed view of the interaction of hMSCs with the nano-HA (10 µg/mL, day 7), showing particles agglomerates over the culture substratum (#), over the cell surface (+) and, apparently, inside the cell (*). B: high magnification image of a nano-HA agglomerate showing the individual nanoparticles. Z1, Z2 and Z3: EDS spectra of the marked areas in the SEM images. A (backscattered image): Bar = 20 µm; B: Bar = 2 µm.

4.2.4 - Cell morphology and F-actin cytoskeletal organization

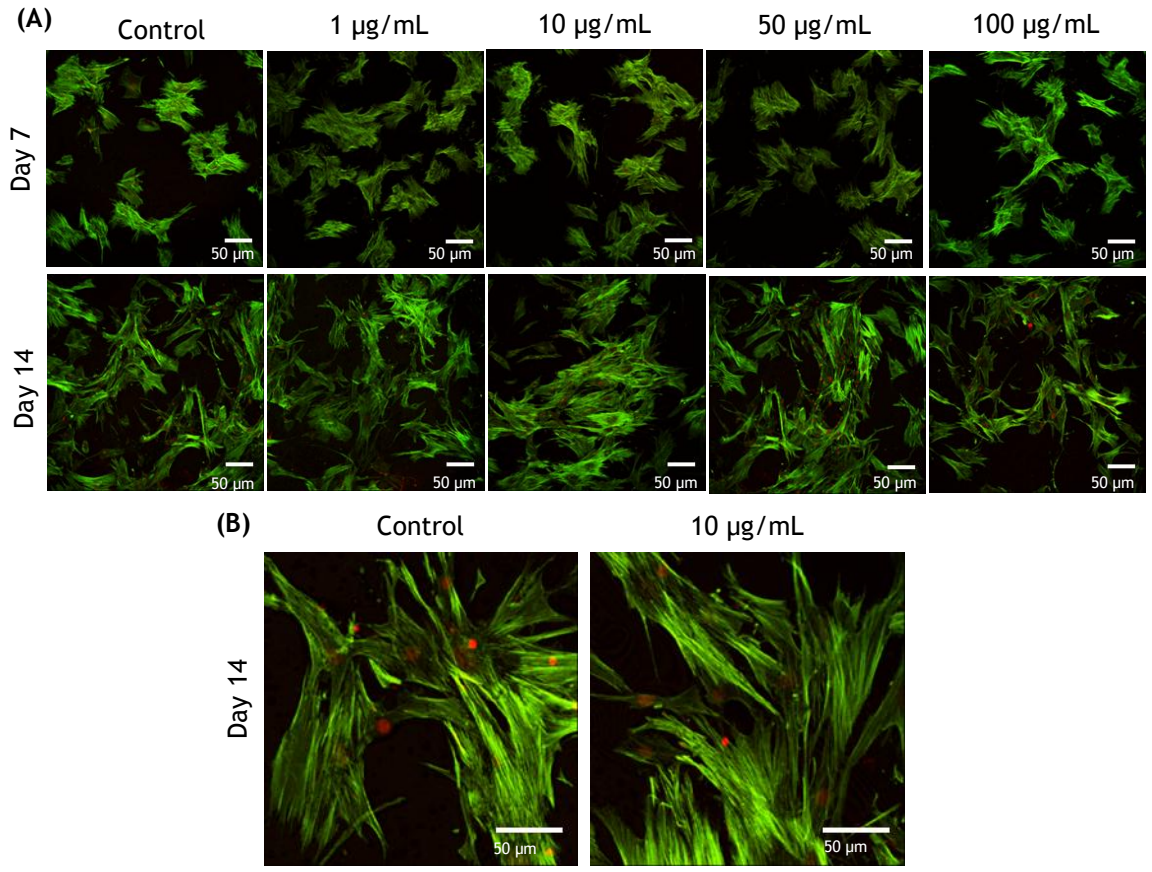

Figure 14 - Confocal laser scanning microscopy images of hMSCs cultured in the absence (control) and in the presence of different nano-HA concentrations (1 to 100 µg/mL), at days 7 and 14 (a). High magnification images of the control cultures and the cultures exposed to 10 µg/mL nano-HA, at day 14 (b). Cultures were stained for actin cytoskeletal organization (green) and nuclei (red). Scale bar = 50 µm.

Confocal laser scanning microscopy (CLSM) allows the observation of the F-actin cytoskeletal organization by staining with fluorescence-labelled phalloidin.

Trough images obtained by CLSM it is possible to assess cell mobility, cell spreading, and cellular morphology. As shown in figure 14 it may be seen that cells displayed an elongated morphology in control and nano-HA 10 µg/mL. In fact when hMSCs were exposed to nano-HA 10 µg/mL showed a normal filamentous morphology and it showed no difference compared with control. In contrast, when cells were exposed to nano-HA 50 and 100 µg/mL cells had alteration in fibres of cytoskeletal.

4.2.5 - Transmission Electron Microscopy (TEM)

Cultures of hMSCs performed in the absence (control) and in the presence of nano-HA were observed by TEM. Figure 15 shows the TEM images for cultures exposed to nano-HA for 1 day. Control cells presented the expected morphology for osteoblastic cells, namely a

prominent nucleus and a rich endoplasmic reticule (figure 15-A). In the presence of nano-HA, a close interaction of the nano-HA aggregates with the cell membrane was observed (figure 15-B, C). Particles were internalized and were located in lysosomic vesicles (figure 15-D, E). Uptake of nano-HA appeared to be dose-dependent, as the cells exposed to 50 µg/mL (figure 15-E) seemed to have a higher amount of internalized particles compared to dose exposed to 10 µg/mL (figure 15-D).

Few cells displaying apoptotic signs were seen in the cultures performed in the presence of 50 µg/mL nano-HA (figure 15-F).

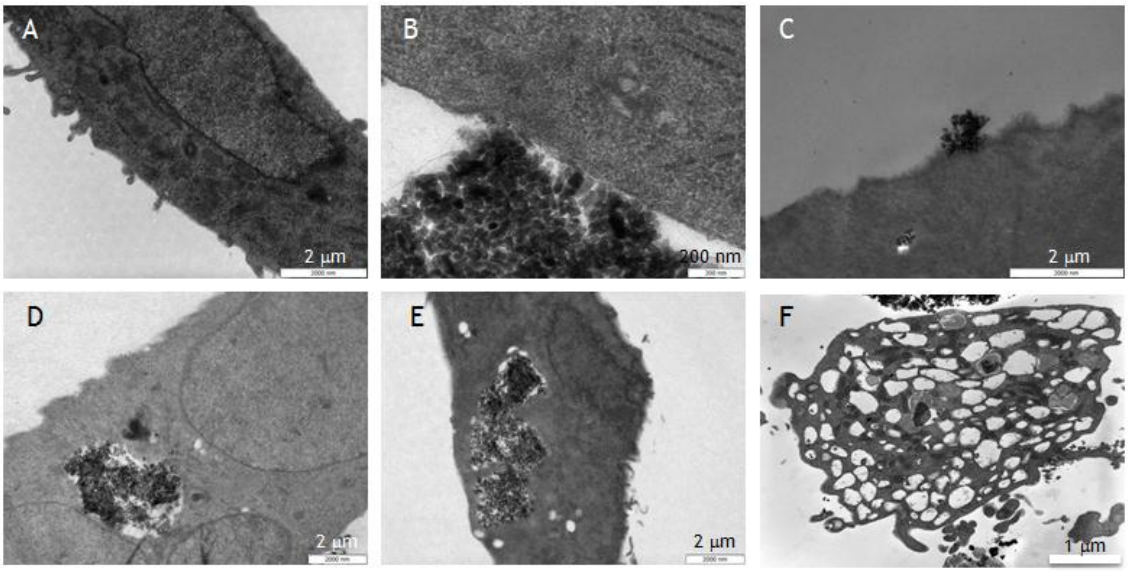

Figure 15 -Transmission electron microscopy images of hMSCs cultured in the absence (control) and in the presence of nano-HA, at day 7, i.e. 1 day after the addition of nano-HA. A: control cell; B and C: interaction of nano-HA with the cell membrane; D: internalized particles in a cell exposed to 10 µg/mL nano-HA; E: internalized particles in a cell exposed to 50 µg/mL nano-HA; F: apoptotic cell found in the cultures exposed to 50 µg/mL nano-HA.

4.2.6 - Apoptosis

Caspase activity is the hallmark for apoptosis. Thus, hMSCs cultured in the absence (control) and in the presence of nano-HA (1 to 100 µg/mL) were assessed for caspase-3 activity (figure 16).

A small increase in the amount of caspase-3 was noted in the cultures exposed to 50 and 100 µg/mL nano-HA, at days 7 and 14 (~16 to 20%). At day 21, values were similar to those on control cultures.

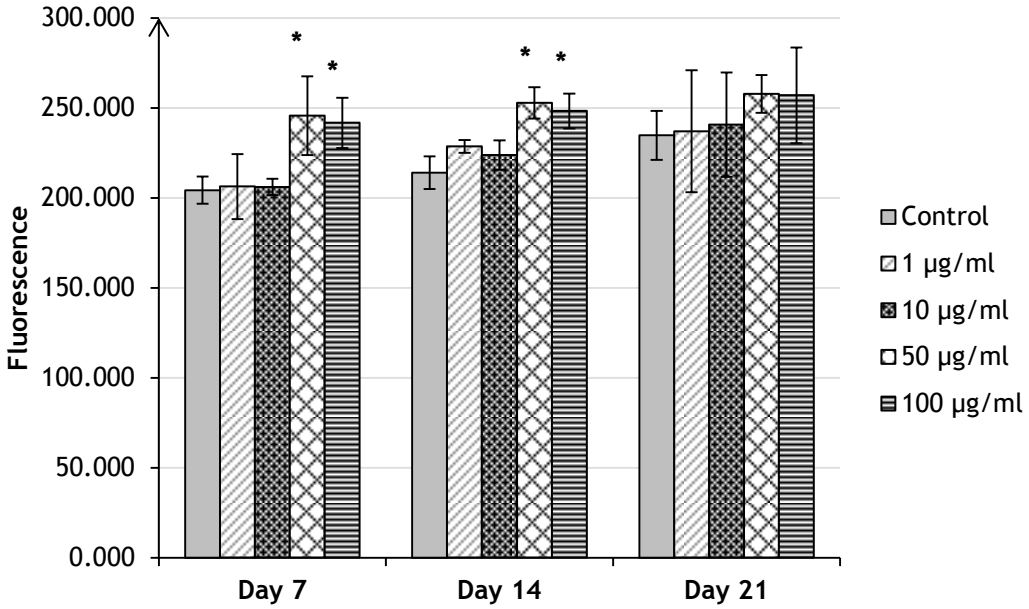

Figure 16 - Apoptosis profile of hMSCs cultured in the absence (control) and in the presence of nano-HA (1 to 100 µg/mL), by the evaluation of the amount of caspase-3, at days 7, 14 and 21. Results were expressed as means ± standard deviation (SD). Asterisks (*) indicate a significant difference ($p < 0.05$) from control (absence of nano-HA).

4.2.7. Gene expression by reverse-transcription polymerase chain reaction (RT-PCR)

The interaction of nano-HA with hMSCs was evaluated for the level of gene expression of osteoblastic-related proteins, such as Runx-2, Col-1, ALP, BMP-2 and OPG .

Figure 17 shows that hMSCs expressed the tested genes. Nano-HA did not significantly affect the expression of Runx-2, Col-1 and OPG. However, nano-HA, at 10 µg/mL, caused a small induction in the expression of BMP-2, at days 7 and 14. In addition, the presence of nano-HA, at 50 µg/mL, resulted in a small decrease in the expression of ALP at days 7 and 21.

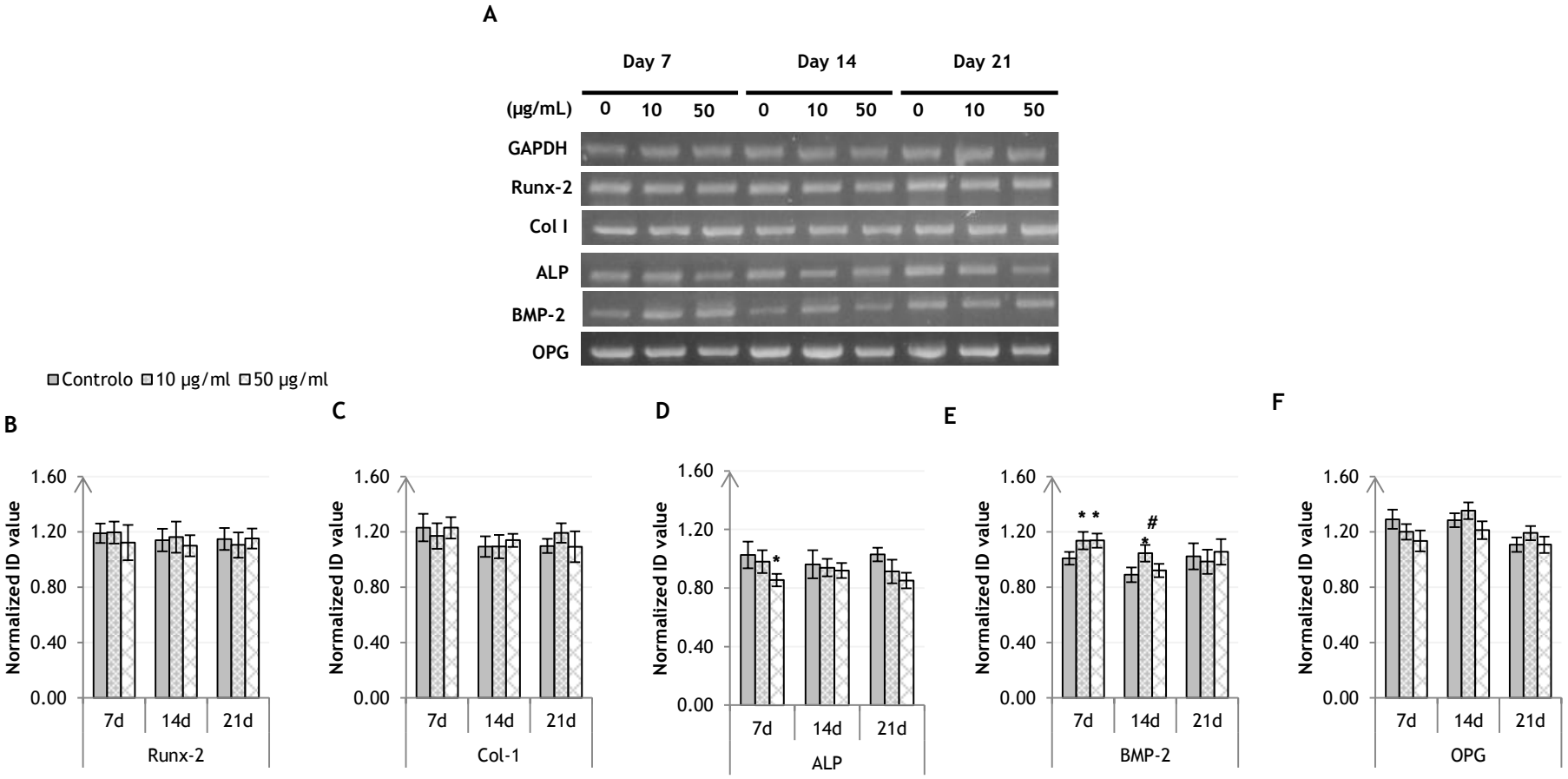

Figure 17 - RT-PCR analyses of hMSCs cultured in the absence (control) and in the presence of nano-HA 10 and 50 µg/mL, at days 7, 14 and 21. Bands of the RT-PCR products (A) were subjected to a measurement of the area and integrated density (ID) by ImageJ 1.41 software. The ID values of gene expression were normalized to the corresponding GAPDH ID value. The expression profile of hMSCs was evaluated for Runx-2 (B), Col-1 (C), ALP (D), BMP-2 and OPG (F). Results were expressed as means ± standard deviation (SD). Asterisks (*) indicate a significant difference ($p < 0.05$) from control and number sign (#) indicate a significant difference between nano-HA 10 and 50 µg/mL.

Chapter 5

Discussion

For bone applications, nano-HA are promising candidates since this structure provides a closer approximation to native bone architecture, compared to micron materials [2, 66]. The decreasing material size leads to modification of the nano featured surfaces, increased surface area, surface roughness and surface to volume ratio, which creates superior physiochemical properties and improved cellular behaviour [1-3, 66, 67, 71]. Thus, strategies based in using nanoparticles to treat/fill bone defects can potentially induce bone formation [102].

The purpose of this investigation was to evaluate the behaviour of hMSCs of a novel synthetic nano-HA - nanoXIM•Hap102® - regarding relevant cellular and molecular events involved in the proliferation and osteoblastic differentiation pathway throughout a 21day culture period.

In order to define the appropriate concentration range of nano-HA to evaluate the cell response, a preliminary dose-dependent study was conducted with MG63 osteoblastic cells using a wide concentration range of nano-HA, 1-1000 µg/mL. The osteoblastic cell line MG63 provides a homogeneous, phenotypically stable and proliferative population and shows many phenotypic features of normal osteoblastic cells including hormonal responsiveness and expression of early and late stage osteogenic genes. For these characteristics MG63 cells has been used extensively as an osteoblast cell model for in vitro research [117, 118]. In fact, in the present study, this osteoblast model allowed to assess the dose-effect of nano-HA in the cell viability/proliferation in the wide range of 1-1000 µL/mL and in a short time period (7 days). The results of this preliminary experiment (figure 6) suggested that nano-HA at concentration higher than 500 µg/mL caused a dose-dependent inhibitory effect on cell metabolic activity/proliferation. This observation is in concordance with that reported in a previous study, also using MG63 cells, showing that HA nanoparticles with a similar morphology caused deleterious effects on osteoblastic cells at concentrations higher than 500 µg/mL [119]. Thereby, in this study, the concentration range of 1-100 µg/mL nano-HA was selected to be tested in the more detailed study of the cell response of hMSCs to the nanoparticles.

As already mentioned, the MSCs have the capacity of self-renewal and they are defined as a type of adult stem cells which contribute, in some circumstance, to the regeneration of mesenchymal tissues, once they have the potential for differentiation in multiple lineages, namely into osteogenic tissue [36, 42, 43]. The in vitro expansion of MSCs has been

extensively studied in this sense, since their use in tissue regeneration and engineering offers promising approaches for the therapy of a wide range of trauma and orthopaedic conditions [83]. It is known that nano-HA can influence the behaviour of bone-related cells [1-3, 69, 83, 96]. Thereby, the effects of the nano-HA formulation NanoXIM•HAp102® on hMSCs were assessed for the viability/proliferation profile, apoptosis, cell morphology and pattern of cell growth, expression of osteoblastic genes and uptake of the nanoparticles throughout a period of 21 days.

The MTT assay (figure 7), which is based in the reducing ability of metabolic active cells, showed time and dose-dependent effects of nano-HA. At day 7, i.e. one day after the addition of the particles, values showed a tendency for a dose-dependent increase in the metabolic activity, which is probably an attempt of the cells in coping with the changes that were imposed to their surroundings due to the presence of the nanoparticles. However, at longer exposure times, MTT assay assessed at day 14 showed a slight dose-dependent decrease in the cell metabolic activity/proliferation suggesting a deleterious effect of nano-HA. Still, with the continuous exposure to the particles, cells were able to recover from this effect at the lower nano-HA levels (1 and 10 μg/mL), as shown by the MTT assay at day 21; in addition, an inductive effect was even observed in the cultures grown in the presence of 10 μg/mL. Higher levels, ≥ 50 μg/mL, caused decreased cell viability/proliferation. These observations are in line with previous studies showing dose-dependent effects of HA nanoparticels in the proliferation of MSCs, including increased proliferation in the presence of nanophase hydroxyapatite particles at concentrations lower than 20 μg/mL [120]. In the present work, it is interesting to note that hMSCs were more sensitive to the deleterious effects of nano-HA compared to MG63 cells. This might be due to the different features of the two cell types, namely related with the more proliferative and uncontrolled growth of MG63 cells compared to that of MSCs [118].

The effect of nano-HA on the osteoblastic differentiation of hMSCs was investigated by histochemical staining for ALP and collagen (figures 8-10). ALP detection was habitually used as an early marker of osteoblast differentiation in vitro; moreover collagen was also widely used to evaluate the osteogenic differentiation of MSCs [46, 64]. Results showed that cells synthetized ALP and collagen and that the cell layer and the staining intensity increased with the culture time. In addition, it was observed that cells grew with a typical organization, namely forming cell clusters that increased progressively and stained intensively. This is a relevant finding, as it is known to be the normal pattern of cell growth of MSCs. Formation of cell clusters is an early and critical event leading to the osteoblastic differentiation and mineralization process [31, 121]. The presence of nano-HA did not affect this pattern of cell growth. However, it is worth to mention that the continuous exposure to nano-HA 10 μg/mL resulted in an increase in the amount of the cell layer and also in the staining intensity for ALP and collagen (mostly at day 21), suggesting an enhanced osteogenic differentiation of MSCs. On the other hand, in the presence of nano-HA 50 μg/mL deleterious effects were observed, reflected by a less abundant cell layer.

SEM observation of the cultures showed that hMSCs were able to attach, spread and proliferate, in control and in the presence of nano-HA, which is in agreement to that observed in the histochemical staining and with results of cell morphology and F-actin cytoskeletal organization. Cells also display the typical elongated/polygonal morphology of the MSCs with long cytoplasmic projections, and a cell layer with abundant cellular interactions (figure 11). SEM images also showed that the nano-HA organized as micrometric

aggregates that appeared to present a high affinity to the cell layer (figures 11 to 13). These aggregates were found in association or in close proximity with the spread cells, and they also appeared to be localized inside the cells (figure 13). EDS spectra of the aggregates confirm the elemental composition of nano-HA, showing the Ca and P peaks.

By using TEM analyses, it was found that nano-HA has a close interaction with the cell membrane and followed an internalization process by an endocytosis pathway, as expected for the uptake of nanoparticles [5, 68, 104, 106-108]. Thereby nano-HA was present in the intracellular environment located in varying size lysosomic vesicles. Moreover, TEM images showed suggested a dose-dependent uptake, as the cultures exposed to nano-HA 50 μg/mL presented a higher amount of internalized particles compared to that seen in the cultures exposed to nano-HA 10 μg/mL. Images also show some degradation/dissolution within the acidic environment of the lysosomes. It has been reported that this process might cause an increase of the levels of Ca^{2+} in the cytoplasm, modulating the cellular behaviour, due to the known role of calcium ions in a variety of intracellular pathways. Appropriate levels of Ca^{2+} might be favourable for the osteoblastic proliferation and differentiation [109]. However, previous studies have also suggested that increases in intracellular calcium may promote apoptosis [68, 122, 123]. Related to this, in the present work, TEM images of the cultures exposed to nano-HA 50 μg/mL show the presence of cells displaying typical apoptotic signs (figure 15F). Also, the evaluation of caspase-3 in the cultures (figure 16) showed increased amount of this enzyme in the presence of the higher nano-HA concentrations (50 and 100 μg/mL).

The effect of nano-HA on hMSCs osteogenic differentiation was assessed by PCR analysis regarding the gene expression of osteoblastic-related proteins, such as Runx2, Col I, ALP, BMP-2 and OPG. Both control cultures and cultures exposed to nano-HA expressed these genes, all of them involved in the osteoblastic differentiation pathway. Runx2 is responsible for inducing the osteogenic phenotype at an early stage and also to inhibit the differentiation of MSCs into adipocytes and chondrocytes [13, 65, 67, 69]. Collagen is the main component of the bone extracellular matrix synthesized by osteoblast lineage cells, and has been considered an early bone differentiation marker, which has a role in osteoblast differentiation [31]. ALP is an early osteoblastic differentiation marker widely used to evaluate the in vitro osteogenic differentiation of MSCs [75]. BMP-2 is known to participate in the regulation of cell growth and differentiation, along with the induction of osteogenic progenitor cells in bone defect sites during the healing process [67, 124]. Furthermore BMP-2 and wingless-ints (Wnts) pathways together have a critical role in promote Runx2 expression to promote osteoblast differentiation [13, 69]. Regarding OPG, this molecule has a key role in the cell-to-cell communication between the osteoblasts and the osteoclasts during the bone remodelling, and it is known to be a negative regulator of osteoclastogenesis [67, 76]; however, its role in osteoblast differentiation is still unclear. But more recently *Yu et al. (2011)* showed that OPG expression is associated with preosteoblast maturation and promotes matrix maturation [76]. Nano-HA, at 10 and 50 μg/mL, did not cause statistically significant effects in the expression of Runx2, Col I and OPG. Still, nano-HA clearly had an inductive effect in the expression of BMP-2. Nevertheless, ALP expression was slightly decreased in the presence of nano-HA 50 μg/mL.

Overall, results showed that nano-HA display a low cytotoxicity profile. Only high levels of nano-HA, similar and higher than 50 μg/mL caused slightly deleterious effects on the cell metabolic activity/proliferation, amount of apoptosis and expression of ALP. On the other

hand, the presence of 10 μg/mL resulted in a slight inductive effect on the cell metabolic activity/proliferation and expression of BMP-2. These observations are in line with the reported studies showing low cytotoxicity of HA nanoparticles towards osteoblastic cells, and also their ability to modulate cell proliferation and differentiation events. Thus, upon exposure to nano-HA, increased proliferation was found in bone marrow-derived mesenchymal stem cells [120] and enhanced osteoblastic differentiation features was also observed for these cells [120,125], and also for the osteoblastic cell lines hFOB [107] and MG63[119] However, these studies show a great variability of results, which is expected considering the wide versatility and diversity of the physicochemical properties of the tested particles, the cell system and the experimental protocols.

Chapter 6

Conclusion

In this thesis, the dose-dependent effect of the nano-HA formulation NanoXIMHap102® was evaluated regarding the proliferation and osteogenic differentiation of hMSCs.

In control conditions (absence of nano-HA), hMSCs proliferated throughout a 21-day culture time, presenting the expected cellular organization for mesenchymal stem cells, namely the formation of cell clusters scattered over the culture substratum. On SEM observation, they showed an elongated/polygonal morphology with abundant cell-to-cell contact. Cultures display a positive staining for ALP and collagen, which increased with the culture time, and expressed the osteoblastic-related genes Runx2, ALP, collagen, BMP-2 and OPG.

TEM analyses revealed that nano-HA was readily internalized by hMSCs by endocytosis. Nano-HA aggregates were seen in varying size lysosomes and showed low intracellular dissolution rate. The presence of nano-HA in hMSCs cultures, in the range 1 - 50 μg/mL, caused negligible effects in the cell behavior. In addition, exposure to nano-HA at 10 μg/mL resulted in an increase in the cell viability/proliferation, accompanied by the synthesis of ALP and collagen, and a normal F-actin cytoskeleton organization, without any increase in the apoptosis rate. Moreover, hMSCs presented increased expression of BMP-2, an important osteogenic differentiation marker. The presence of higher nano-HA levels (50 and 100 μg/mL) were associated with slight deleterious effects in the measured cell response parameters.

These data contribute to further understanding of the functional properties of the nano-HA formulation NanoXIM•HAp102®. Accordingly, nano-HA was able to modulate the proliferation and osteoblastic differentiation of hMSCs. At selected conditions, nano-HA exhibits an interesting profile for bone tissue applications.

References

[1] Cardoso D A, Jansen J A, Leeuwenburgh S C G, Synthesis and application of nanostructured calcium phosphate ceramics for bone regeneration. *J Biomed Mater Res B Appl Biomater*, **2012**, 100, 2316–2326.

[2] Zhang L, Webster T J, Nanotechnology and nanomaterials: Promises for improved tissue regeneration. *Nanotoday*, **2009**, 4, 66–80.

[3] Fox K, Tran P A, Tran N, Recent Advantages in Research Applications of Nanophase Hydroxyapatite. *ChemPhysChem2*, **2012**, 13, 2495–2506.

[4] Hench L L, Wilson J, An Introduction to Bioceramics, *World Scientific Publishing Co Pte Ltd*, Chap. 9, **1993**.

[5] Silva V M T M, Quadros P A, Laranjeira P E M S C, Dias M M, Lopes J C B, A Novel Continuous Industrial Process for Producing Hydroxyapatite Nanoparticles, Journal of Dispersion Science and Technology, V. 29, pp. 542–547, 2008.

[6] *Fluidinova*,http://www.fluidinova.com/products/nanoxim-med/nanoxim-hap100/hydroxyapatite-nanoparticles-pastes-for-use-inmedical-applications/62/, **Accessed 10 October 2012**.

[7] Blitterswijk C V, Tissue Engineering, Ed. 1st, Chap. An introduction, *Academic Press,* **2007**.

[8] Saltzman W M, Tissue Engineering: Engineering Principles for the Design of Replacement Organs and Tissues. *OUP USA*, **2004,** 5-16.

[9] GrifÞth L G, Naughton G, Tissue Engineering-Current Challenges and Expanding Opportunities. *Science*, **2002**, 295, 1009-1013.

[10] Dorozhkin S V, Calcium Orthophosphates in Nature, Biology and Medicine. *Materials*, **2009**, 2, 399-498.

[11] Mellon S J, Tanner K E, Bone and its adaptation to mechanical loading: a review. *International Materials Reviews*, **2012,** 57, 235-255.

[12] Pina S, Cements of doped calcium phosphates for bone implantation, *Universidade de Aveiro*, Ph.D.Thesis, Aveiro, **2009**.

[13] Datta H K, Ng W F, Walker J A, Tuck S P, Varanasi S S, The cell biology of bone metabolism. *J Clin Pathol*, **2008**, 61, 577-587.

[14] Blair H C, Zaidi M, Schlesinger P H, Mechanisms balancing skeletal matrix synthesis and degradation. *Biochem J.*, **2002**, 364, 329-341.

[15] Laranjeira M S, Preparation and characterization of porous 3D Bonelike® structures through biomodelling and 3D machining techniques, *Faculdade de Engenharia da Universidade do Porto*, Master thesis, Porto, **2006**.

[16] Wopenka B, Pasteris J D, A mineralogical perspective on the apatite in bone. *Materials Science and Engineering*, **2005**, 25, 131–143.

[17] Karlson M, Nano-porous alumina a potencial bone implant coating, *Uppsala University*, Ph.D.Thesis, Uppsala, **2004**.

[18] Tortora G, Principles of anatomy and physiology, 11th Ed, Chap. 6, *New Jersey: J. Wiley: Hoboken*, **2006**.

[19] Sousa J P, Efeito das BMPs na regeneração óssea: mecanismo de acção e aplicação em Medicina Dentária, *Faculdade de Medicina Dentária da Universidade do Porto*, Dissertação de Mestrado, Porto, 2011.

[20] Mateus A Y P, Development, Characterisation and Application of Calcium Phosphates Nanocrystals Aggregates in a Collagen Matrix to be used as Biomaterial in Bone Regeneration, *Faculdade de Engenharia da Universidade do Porto*, Master thesis, Porto, **2010**.

[21] Downey P A, Siegel M I, Bone Biology and the Clinical Implications for Osteoporosis. *Physical Therapy*, **2006**, 86, 77-91.

[22] Buckwalter J A, Glimcher M J, Cooper RR, Becker R, Bone biology, part I: structure, blood supply, cells, matrix, and mineralization. Cap. 4-7, *Academic Press*, **1996**.

[23] Arnett T, Henderson B, Methods in Bone Biology. Ed. 1 st, Chap. 1, *Springer*, **1997**.

[24] Seibel M J., Robins S P., Bilezikia J P, Dynamics of Bone and Cartilage Metabolism: Principles and Clinical Applications, Ed 2 nd, Chap. 4 and 14, *Academic Press*, **2006**.

[25] Marks S, Popoff S, Bone cell biology: the regulation of development, strucutre and function in the skeleton. *American Journal of Anatomy*, **1988**, 183, 1–44.

[26] Holtrop M E, Light and electron microscopic structure of bone forming cells. *Telford Press Inc*, 1, 1–39, **1990**.

[27] Lian J B, Stein G S, Development of the osteoblast phenotype: molecular mechanisms mediating osteoblast growth and differentiation. *Iowa Orthop J*, **1995**, 15, 118–140.

[28] Frost H M, Dynamics of bone remodeling. *Bone Biodynamics*, **1964,** 315–33.

[29] Bronner F, Farach-Carson M C, Rubin J, Bone Resorption (Topics in Bone Biology), Ed. 1st, Vol 2, Chap. 4, *Springer*, **2005**.

[30] Bonnick S L, Bone Densitometry in Clinical Practice, Ed. 3rd, Cap 2, *Humana Press*, **2009**.

[31] Bilezikian J P, Raisz L G, Martin T J, Principles of Bone Biology,Ed 2 nd, Vol.1, Academic Press, 2002.

[32] Davies J E, Understanding Peri-Implant Endosseous Healing. *Journal of Dental Educatio*, **2005**, 67, 932-949.

[33] Sela J J, Bab I A, Principles of Bone Regeneration, Ed. 1st, Chap. 1, Springer, **2012**.

[34] Lieberman J R, Friedlaender G E, Bone Regeneration and Repair: Biology and Clinical Applications, Ed. 1st, Chap.2, *Humana Press*, **2005**.

[35] Braddock M, Houston P, Campbell C, Ashcroft P. Born again bone: Tissue engineering for bone repair. *News Physiol. Sci.*, **2001**, 208-213.

[36] Nolta J A, Genetic Engineering of Mesenchymal Stem Cells, Chap. 1, *Springer*, **2006**

[37] Atala A, Lanza B, Methods of Tissue Engineering, Chap. 26, *Academic Press Inc*, **2001**.

[38] Bajada S, Mazakova I, Ashton B A, Richardson J B, Ashammakhi N, Stem Cells in Regenerative Medicine: Topics in Tissue Engineering. Vol. 4, Chap. 13, *F Chiellini*, **2008**.

[39] Marshak D R, Gardner R L, Gottlieb D, Stem Cell Biology, Chap. 16, *Cold Spring Harbor Press*, **2001**.

[40] Beresford J N, Owen M E, Marrow Stromal Cell Culture, *Cambridge University Press*, **1998**.

[41] Amaral I, Chitosan Matrices for Cell-based Bone Regenerative Therapies, *Faculdade de Engenharia da Universidade do Porto*, Ph.D.Thesis, Porto, **2005**.

[42] Watt F M, Driskell R R, The therapeutic potential of stem cells, Phil. *Trans. R. Soc. B*, **2010,** 365, 155–163.

[43] Turksen K, Adult and Embryonic Stem Cells, Chap. 2, *Humana Press*, **2012**.

[44] Meyer U, Meyer T, Handschel J, Wiesmann H P, Fundamentals of Tissue Engineering and Regenerative Medicine, Chap. 41, *Springer*, **2009**.

[45] Coelho M J, Fernandes M H, Human bone cell cultures in biocompatibility testing. Part II: effect of ascorbic acid, ß-glycerophosphate and dexamethasone on osteoblastic differentiation. *Biomaterials*, **2000,** 21, 1095-1102.

[46] Bhattacharya N, Stubblefield P, Frontiers of Cord Blood Science, Chap. 5, *Springer*, **2009**.

[47] Komori T, Regulation of Osteoblast Differentiation by Transcription Factors. *Journal of Cellular Biochemistry*, **2006**, 99, 1233–1239.

[48] Jacobi A, Rauh J, Bernstein P, Liebers C, Zou X, Comparative analysis of reference gene stability in human mesenchymal stromal cells during osteogenic differentiation. *Biotechnology Progress,* **2013**.

[49] Neve A, Corrado A, Cantatore F P, Osteoblast physiology in normal and pathological conditions. *Cell Tissue Res*, **2011**, 343, 289–302.

[50] Deng Z L, Sharff K A, Tang N et al. Regulation of osteogenic differentiation during skeletal development. *Frontiers in Bioscience*, **2008**, 13, 2001-21.

[51] Komori T, Regulation of Skeletal Development by the Runx Family of Transcription Factors. *Journal of Cellular Biochemistry*, **2005**, 95, 445–453.

[52] Fisher J P, Tissue Engineering Advances in Experimental Medicine and Biology. Ed. 1 st, 433-438, *Springer,* **2007.**

[53] Kassem M, Abdallah BM, Saeed H, Osteoblastic cells: differentiation and trans-differentiation. *Arch Biochem Biophys*, **2008**, 473, 183–187.

[54] Kulterer B, Friedl G, Jandrositz A, Sanchez-Cabo F, Prokesch A, Paar C, Scheideler M, Windhager R, Preisegger KH, Trajanoski k, Gene expression profiling of human mesenchymal stem cells derived from bone marrow during expansion and osteoblast differentiation. *BMC Genomics,* **2007**, 8, 70-82.

[55] Roman-Roman S, Garcia T, Jackson A, Theilhaber J, Rawadi G, Connolly T, Spinella-Jaegle S, Kawai S, Courtois B, Bushnell S, Auberval M, Call K, Barona R, Identification of genes regulated during osteoblastic differentiation by genome-wide expression analysis of mouse calvaria primary osteoblasts in vitro. *Bone* **2003**, 32, 474–482.

[56] Birmingham E, Niebur G L, McHugh P E, Shaw G, Barry F P, McNamara L M, Osteogenic differentiation of mesenchymal stem cells is regulated by osteocyte and osteoblast cells in a simplified bone niche. *Eur Cell Mater*, **2012**, 23, 13-27.

[57] Yu H, Vos P, Ren Y, Overexpression of osteoprotegerin promotes preosteoblast differentiation to mature osteoblasts. *Angle Orthodontist*, **2011**, 81, 100-106.

[58] Logan J, Edwards K, Saunders N, Real-time PCR: Current Technology and Applications. Ed. 1 st, Chapter 9, *Caister Academic Press*, **2009.**

[59] Bagasra O, Hansen J, In-Situ PCR Techniques. Ed. 1 st, Chapter 1, *Wiley-Liss*, **1997**.

[60] Mullis K B, Faloona F A, Specific synthesis of DNA in vitro via a polymerase catalysed chain reaction. *Methods Enzymol*, **1987**, 155, 335-50.

[61] Peake I, The polymerase chain reaction. *J Clin Pathol*, **1989**, 42, 673-676.
[62] Lynch J R, Brown J M, The polymerase chain reaction: current and future clinical applications. *Med Genet*, **1990**, 27, 2-7.
[63] Andersen C L, Jensen J L, Ørntoft T F, Normalization of Real-Time Quantitative Reverse Transcription-PCR Data: A Model-Based Variance Estimation Approach to Identify Genes Suited for Normalization, Applied to Bladder and Colon Cancer Data Sets. *Cancer Research*, **2004**, 64, 5245–5250.
[64] Tristan C, Shahani N, Sedlak T W, Sawa A, The diverse functions of GAPDH: Views from different subcellular compartments. *Cellular Signalling*, **2011**, 23, 317–323.
[65] Chen H, Zeng Y, Liu W, Zhao S, Wu J, Du Y, Multifaceted applications of nanomaterials in cell engineering and therapy. *Biotechnol Adv*, **2012**.
[66] McMahon R E, Wang L, Skoracki R, Mathur A B, Development of nanomaterials for bone repair and regeneration. *J Biomed Mater Res Part B*, **2013**, 101, 387–397.
[67] Webster T J, Ergun C, Doremus R H, Siegel R W, Bizios R, Enhanced osteoclast-like cell functions on nanophase ceramics. *Biomaterials,* **2001,** 22, 1327–1333.
[68] Motskin M, Wright D M, Muller K, Kyle N, Gard T G, Porter A E , Skepper J N, Hydroxyapatite nano and microparticles: Correlation of particle properties with cytotoxicity and biostability. *Biomaterials*, **2009,** 30, 3307–3317.
[69] Ferraz M P, Monteiro F J, Manuel C M, Hydroxyapatite nanoparticles: A review of preparation methodologies. *Journal of Applied Biomaterials & Biomechanics*, **2004**, 2, 74-80.
[70] Liou S, Chen S, Liu D, Synthesis and characterization of needlelike apatitic nanocomposite with controlled aspect ratios. *Biomaterials*, **2003**, 24, 3981–3988.
[71] Webster T J, Siegel R W, Bizios R, Osteoblast adhesion on nanophase ceramics. *Biomaterials*, **1999**, 20, 1221–1227.
[72] Guo X, Gough J E, Xiao P, Liu J, Shen Z, Fabrication of nanostructured hydroxyapatite and analysis of human osteoblastic cellular response. *J Biomed Mater Res A*, **2007**, 82, 1022-32.
[73] Webster T J, Ergun C, Doremus R H, Siegel R W, Bizios R, Specific proteins mediate enhanced osteoblast adhesion on nanophase ceramics. *J Biomed Mater Res*, **2000**, 51, 475-48.
[74] Gomes P J, Silva V M T M, Quadros P A, Dias M M, Lopes, J C B, A Highly Reproducible Continuous Process for Hydroxyapatite Nanoparticles Synthesis. *J Nanosci Nanotechnol,* **2009**, 9, 3387-95.
[75] Brown P W, Calcium Phosphates in Biomedical Engineering. *Encyclopedia of Materials: Science and Technology*, **2001**, 893–897.
[76] Hench L L, Wilson J, An Introduction to Bioceramics, *World Scientific Publishing Co Pte Ltd*, Chap. 9, **1993**.
[77] Uskokovic´ V, Uskokovic´D P, Nanosized hydroxyapatite and other calcium phosphates: Chemistry of formation and application as drug and gene delivery agents. *J Biomed Mater Res B Appl Biomater,* **2011**, 96, 152-91.
[78] White A A, Production and characterization of hydroxyapatite/ multi-welled carbon nanotube composites. *Clare college University of Cambridge*, Ph.D. Thesis, Cambridge, **2009**.
[79] Poinern G E, Brundavanam R K, Mondinos N, Jiang Z T, Synthesis and characterisation of nanohydroxyapatite using an ultrasound assisted method. *Ultrason Sonochem*, **2009**, 16, 469–474.

[80] Legeros R Z, Biodegradation and bioresorption of calcium phosphate ceramics. *Clin Mater*, **1993**, 14, 65–88.

[81] Zhou H, Lee J, Nanoscale hydroxyapatite particles for bone tissue engineering. **Acta Biomaterialia**, **2011**, 7, 2769–2781.

[82] Dolatshahi-Pirouz A, Jensen T, Foss M, Chevallier J, Besenbacher F, Enhanced Surface Activation of Fibronectin upon Adsorption on Hydroxyapatite. *Langmuir*, **2009**, 25, 2971-2978.

[83] Cai Y, Liu Y,Yan W,Hu Q, Tao J, Zhang M, Shic Z, Tang R, Role of hydroxyapatite nanoparticle size in bone cell proliferation. *J Mater Chem*, **2007**, 17, 3780–3787.

[84] Balasundarama G, J. Webster T J, A perspective on nanophase materials for orthopedic implant applications. *J Mater Chem*, **2006**, 16, 3737–3745.

[85] Rhee S, Synthesis of hydroxyapatite via mechanochemical treatment. *Biomaterials*, **2002**, 23, 1147–1152.

[86] Bouyer E, Gitzhofer F, Boulos MI, Morphological study of hydroxyapatite nanocrystal suspension. *J Mater Sci Mater Med*, **2000**, 11, 523-31.

[87] Afshara A, Ghorbania M, Ehsania N, Saeria M R, Sorrell C C, Some important factors in the wet precipitation process of hydroxyapatite. *Materials and Design*, **2003**, 24, 197–202.

[88] Santos M H, Oliveira M, Souza L P F,Mansur H S, Vasconcelos W L, Synthesis Control and Characterization of Hydroxyapatite Prepared by Wet Precipitation Process. *Materials Research*, **2004**, 7, 625-630.

[89] Lopes J C B, Laranjeira P E M S C, Dias M M Q. Martins A A A, Network Mixer and Related Mixing Process. WO Patent **2005**/077508.

[90] Fluidinova, http://www.fluidinova.com/main.php?id=32, **Accessed 16 January 2013**.

[91] Faria R P V, Estudo e Optimização do Processo Industrial de Produção de Hidroxiapatite Recorrendo à Tecnologia NETmix®. *Faculdade de Engenharia da Universidade do Porto,* Master thesis, Porto, **2008**.

[92] Laranjeira P E M S C, NETmix® Static Mixer- Modeling, CDF Simulation and Experimental Chatacterisation. *Faculdade de Engenharia da Universidade do Porto*, Ph.D. Thesis, Porto, **2005**.

[93] Correia Daniela, Production of Hydroxyapatite Nanoparticles for Cosmetic and Orthopaedic Applications: Effect of Chelants and Dispersants. *Faculdade de Engenharia da Universidade do Porto,* Master thesis, Porto, **2008**.

[94] Rodrigues M F B, Doping of Hydroxyapatite Nanoparticles with Metal Ions for Biomedical, Orthopaedic and Dentistry Applications. *Faculdade de Engenharia da Universidade do Porto*, Master thesis, Porto, **2008**.

[95] Kalita S J, Bhardwaj A, Bhatt H A, Nanocrystalline calcium phosphate ceramics in biomedical engineering. *Materials Science and Engineering C*, **2007**, 27, 441–449.

[96] Puleo D A, Nanci A, Understanding and controlling the bone-implant interface. *Biomaterials*, **1999**, 20, 2311-2321.

[97] Kumta, P N, Sfeir C, Lee D-H, Nanostructured calcium phosphates for biomedical applications: novel synthesis and characterization. *Acta Biomaterialia*, **2005**, 1, 65-83.

[98] Phillips M J, Darr J A, Luklinska Z B, Rehman I, Synthesis and characterization of nano-biomaterials with potential osteological applications. *J Mater Sci Mater Med*, **2003**, 14, 875-82.

[99] Huang S B, Gao S S, Yu H Y, Effect of nano-hydroxyapatite concentration on remineralization of initial enamel lesion in vitro. *Biomed. Mater*, **2009**, 4, 1-6.

[100] Wu H-C, Wang T-W, Sun J-S, Wang W-H, Lin F-H, A novel biomagnetic nanoparticle based on hydroxyapatite. *Nanotechnology*, **2007**, 18, 165601-165609.

[101] Tran N, Webster T J, Nanotechnology for bone materials. *Wiley Interdiscip. Rev. Nanomed. Nanobiotechnol*, **2009**, 1, 336–351.

[102] Tran N, Webster T J, Increased osteoblast functions in the presence of hydroxyapatite-coated iron oxide nanoparticles *Acta Biomater*, **2011**, 7, 1298-306.

[103] Tran N, Webster T J, Magnetic nanoparticles: biomedical applications and challenges. *J Mater Chem*, **2010**, 20, 8760–8767.

[104] Verma A, Stellacci F, Effect of Surface Properties on Nanoparticle–Cell Interactions. *Small*, **2010**, 6, 12–21.

[105] Webster T J, Nanophase ceramics: The future orthopedic and dental implant materials. *Adv Chem Eng*, **2001**, 27, 125–166.

[106] Bauer I W, Li S-P, Han Y-C, Yuan L, Jin M-Z, Internalization of hydroxyapatite nanoparticles in liver cancer cells. *J Mater Sci Mater Med.*, **2008**, 19, 1091-5.

[107] Xu J L, Khor K A, Sui J J, Zhang J H, Chen W N, Protein expression profiles in osteoblasts in response to differentially shaped hydroxyapatite nanoparticles. *Biomaterials*, **2009**, 30, 5385-5391.

[108] Shi Z, Huang X, Cai Y, Tang R, Yang D. Size effect of hydroxyapatite nanoparticles on proliferation and apoptosis of osteoblast-like cells. *Acta Biomaterialia*, **2009**, 5, 338-345.

[109] Maeno S, Niki Y, Matsumoto H, Morioka H, Yatabe T, Funayama A, The effect of calcium ion concentration on osteoblast viability proliferation and differentiation in monolayer and 3D culture. *Biomaterials*, **2005**, 26, 4847–55.

[110] Elmore S, Apoptosis: A Review of Programmed Cell Death. *Toxicologic Pathology*, **2007**, 35, 495–516.

[111] Kerr J F R, Whyllie A H, Currie A R, Apoptosis: A basic biological phenomenon with wide-ranging implications in tissue kinetics. *Br. J. Cancer*, **1972**, 26, 239-257.

[112] Watanabe M, Hitomi M, van der Wee K, Rothenberg F, Fisher S A, Zucker R, Svoboda K K, Goldsmith E C, Heiskanen K M, Nieminen A L, The pros and cons of apoptosis assays for use in the study of cells, tissues, and organs. *Microsc Microanal*, **2002,** 8, 375-91.

[113] Haunstetter A, Izumo S. Apoptosis: basic mechanisms and implications for cardiovascular disease. *Circ Res.* **1998**, 82, 1111-29.

[114] Lincz L F, Deciphering the apoptotic pathway: All roads lead to death. *Immunology and Cell Biology*, **1998**, 76, 1-19.

[115] Porter A G, Jänicke R U. Emerging roles of caspase-3 in apoptosis. *Cell Death Differ*, **1999**, 6, 99-104.

[116] Nicholson D W, Ali A, Thornberry N A, Identification and inhibition of the ICE/CED-3 protease necessary for mammalian apoptosis. *Nature,* **1995**, 43, 376-7.

[117] Hattar S, Berdal A, Asselin A, Loty S, Greenspan D C, Sautier J M; Behaviour of moderately differentiated osteoblast-like cells cultured in contact with bioactive glasses. *European Cells and Materials*, **2002**, 4, 61-69.

[118] Czekanska E M, Stoddart M J, Richards R G, Hayes J S; In search of an osteoblast cell model for *in vitro* research. European *Cells and Materials,* **2012**, 24, 1-17.

[119] Santos C, Gomes P S, Duarte J A, Franke R, Almeida M M, Costa M E V, M H, Fernandes; Relevance of the sterilization-induced effects on the properties of different hydroxyapatite nanoparticles and assessment of the osteoblastic cell response. *Journal of the Royal Society Interface*, **2012**, 9, 3397-3410.

[120] Liu Y, Wang G, Cai Y, Ji H, Zhou G, Zhao X, Tang R, Zhan M; In vitro effects of nanophase hydroxyapatite particles on proliferation and osteogenic differentiation of bone marrow-derived mesenchymal stem cells. *Journal of Biomedical Materials Research Part A*, **2008,** 1083-1091.

[121] Gao Y, Cao W-L, Wang X-Y, Gong Y-D, Tian J-M Zhao N-M, Zang X-F; Characterization and osteoblast-like cell compatibility of porous scaffolds: bovine hydroxyapatite and novel hydroxyapatite artificial bone. *J Mater Sci Mater Med,* **2006**, 17, 815–823.

[122] Yu S P, Canzoniero L M T, Choi D W; Ion homeostasis and apoptosis. *Curr Opin Cell Biol*, **2001**,13, 405–411.

[123] Wang L, Zhou G, Liu H, Niu X, H J, Zhengac L, Fan Y; Nano-hydroxyapatite particles induce apoptosis on MC3T3-E1 cells and tissue cells in SD rats. *Nanoscale*, **2012**, 4, 2894–2899.

[124] Kim K, Dean D, Lu A, Mikos A G, Fisher J P, Early osteogenic signal expression of rat bone marrow stromal cells is influenced by both hydroxyapatite nanoparticle content and initial cell seeding density in biodegradable nanocomposite scaffolds. *Acta Biomaterialia*, **2011**, 7, 1249–1264.

[125] Gonzalez-McQuire R, Green D W, Partridge K A, Oreffo R O C, Mann S, Davis S A; Coating of Human Mesenchymal Cells in 3D Culture with Bioinorganic Nanoparticles Promotes Osteoblastic Differentiation and Gene Transfection *Advanced Materials*, **2007**, 19, 2236-2240.

Annex 1

Technical datasheet of NanoXIM•Hap102®

Technical Datasheet

nanoXIM•HAp102

nanoXIM•HAp102 is an highly pure nanocrystalline hydroxyapatite, supplied as 15±1% wt. paste, with no other additives. This paste is formed by nanocrystals with an aspect ratio of 1:10 (Figure 1).

Table I. nanoXIM•HAp102 main characteristics.

Aqueous Product	Content	Size (TEM) (nm)
nanoXIM•HAp102	15%wt. paste	<100

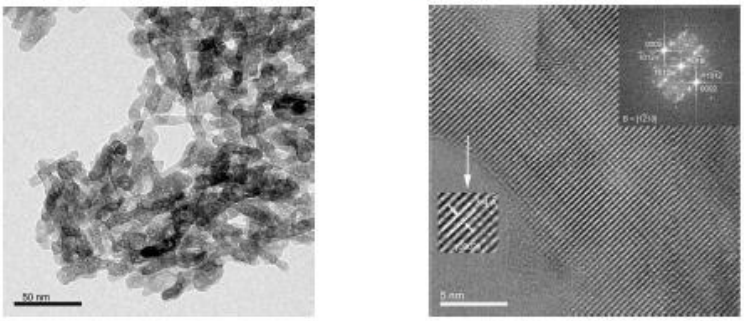

a b

Figure 1. a) High Resolution TEM image of nanoXIM·HAp102 particles presenting thumb shape, 30 nm length and 3 nm of diameter. b) Crystal oriented along the [0002] zone axis illustrating the regularity of the repeating pattern. Right inset shows the FFT, pattern of the hexagonal crystal shape *

* HRTEM Microscope JEOL 2010F operated at 200 kV, bright-field images with courtesy of Prof Paulo Ferreira, Materials Science and Engineering Program, University of Texas at Austin.

The **nanoXIM•HAp102** product is a synthetic calcium phosphate with a single hydroxyapatite phase. Figure 2a shows an X-ray diffractogram of a non-calcinated dried sample, distinctive of the single presence of HAp. This special quality of **nanoXIM•HAp102** is further established since even for calcination temperatures above 1000ºC (Figure 2b) no trace of other phases can be detected.

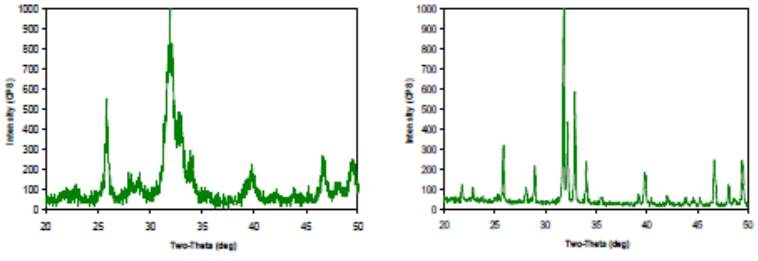

a b

Figure 2. X-ray diffraction diffractgram of **nanoXIM•HAp102**, a) without thermal treatment and b) with thermal treatment to 1250ºC

The purity of **nanoXIM•HAp102** is shown by the extremely low heavy-metal contents present in the hydroxyapatite, significantly lower than limits fixed by the **ISO 13779-1** and **ASTM F1185-03** standards (Table II).

Table II. Comparision of the heavy-metal content in hydroxyapatite limits fixed by the **ISO 13779-1** and **ASTM F1185-03** and values obtained for **nanoXIM•HAp**.

	Element (ppm)			
	As	**Hg**	**Cd**	**Pb**
ISO 13779-1 / ASTM F1185-03	**3**	**5**	**5**	**30**
nanoXIM•HAp	**< 0.1**	**< 0.05**	**< 0.05**	**0.5**

High BET specific surface area is observed for **nanoXIM•HAp102**, with values higher than 80 m^2/g for oven-dried particles obtained consistently and guaranteed.

ICP analysis, *Inductively Coupled Plasma,* systematically detects a stoichiometric ratio between Calcium and Phosphorous (Ca/P) of 1.67±1%, verifying the precise and controlled **nanoXIM•HAp** stoichiometric reaction formulation under production.

Storage Conditions:

Storage of **nanoXIM•HAp102** suspension should follow standard, good-practice storage procedures. After a long period of storage, the suspension may present some settling. Shaking or stirring the product before use is recommended in order to obtain good homogenisation. The storage must be in a clean and dry place at room temperature. Avoid freezing.

Safety:

For detailed information on safety conditions and procedures please refer to the **nanoXIM•HAp – Hydroxyapatite suspension** Material Safety Data Sheet (MSDS).

For additional information on this and other **nanoXIM•HAp** products please contact the Technical Department at Fluidinova S.A.

All the enclosed data is based on our technical experience and on laboratory studies. The product behaviour may vary according to its final application. Handling of this product may be subjected to multiple factors for which Fluidinova is not answerable.

Fluidinova, Engenharia de Fluidos, SA
TECMAIA - Rua Engº Frederico Ulrich, nº 2650
4470-605 Moreira da Maia – Portugal
Tel: +351 229 408 265 | Fax: +351 229 408 266
E-mail: geral@fluidinova.pt